The Canadian Mineralogist
Vol. 44, pp. 000 (2006)

THE PETROGENESIS AND TECTONIC SETTING OF ULTRAMAFIC ROCKS FROM ITI AND KALLIDROMON MOUNTAINS, CONTINENTAL CENTRAL GREECE: VESTIGES OF THE PINDOS OCEAN

SOFIA KARIPI[§], BASILIOS TSIKOURAS AND KONSTANTIN HATZIPANAGIOTOU

Department of Geology, Section of Earth Materials, University of Patras, GR-265 00 Patras, Greece

ABSTRACT

The Iti and Kallidromon ophiolites, in continental central Greece, consist mainly of an ophiolite mélange overthrust by variably serpentinized ultramafic rocks. They include lherzolite and harzburgite; dunite pods occur within the lherzolite at Kallidromon. All rock types display typical textures of Alpine-type mantle rocks. Spinel, olivine and pyroxene compositions are similar to analogous phases from oceanic peridotites. The lherzolite contains an aluminous spinel. The dunite and harzburgite contain two compositional variants of Cr-rich spinels, both commonly present in zoned grains, one with higher Cr# and a second with lower Cr#. Linear variations of Al_2O_3, CaO, V and Ni with MgO, coupled with incompatible and rare-earth-element depletion and mineral compositions, suggest prior events of partial melting in both the lherzolite and harzburgite. The LREE enrichment in the harzburgite, as well as the development of Cr-rich spinel and tremolite and the PGE distribution in both the dunite and harzburgite, are consistent with a history of melt–peridotite interaction. The melt is considered to have been of boninitic composition, generated in the mantle wedge above a subduction zone. The harzburgite was formed at values of smaller melt:rock ratio relative to the dunite owing to partial assimilation of clinopyroxene and orthopyroxene from the host lherzolite. The dunite is considered to have been formed by assimilation of clinopyroxene and orthopyroxene, and replacement of Al-rich spinel by Cr-rich spinel, when locally ponded boninitic melts reacted with the host lherzolite. In both the harzburgite and dunite, subsequent differentiation of magma resulted in the formation of compositional areas poorer in Cr in the spinel grains. The involvement of a boninitic melt and the significant contribution of H_2O in the formation of the harzburgite and dunite, along with mineralogical evidence, particularly Fo- and Cr-rich olivine in the dunite and high-Cr spinel in both the dunite and harzburgite, suggest a subduction-related regime for the origin of the Iti and Kallidromon ophiolites. Moreover, covariation of Cr/Al and Ni/Al values similar to the well-known SSZ-type ophiolites of Vourinos support the above hypothesis.

Keywords: ophiolite, ultramafic rocks, rare-earth elements, platinum-group elements, melt–peridotite interaction, Iti, Kallidromon, Greece.

SOMMAIRE

Les massifs ophiolitiques de Iti et Kallidromon, en Grèce continentale centrale, contiennent surtout un mélange ophiolitique recouvert par chevauchement par des roches ultramafiques à degré de serpentinisation variable, par exemple lherzolite et harzburgite; des lentilles de dunite sont présentes dans la lherzolite à Kallidromon. Toutes les roches font preuve de textures typiques de roches mantelliques de type alpin. Les compositions de spinelle, olivine et pyroxene ressemblent aux phases analogues de péridotites océaniques. La lherzolite contient un spinelle alumineux, La dunite et la harzburgite contiennent de variantes de spinelle chromifère, les deux généralement présents dans les grains zonés, un avec une valeur de Cr# élevée, et l'autre ayant une valeur plus faible. D'après les variations linéaires en Al_2O_3, CaO, V et Ni avec MgO, couplées avec les niveaux appauvris d'éléments incompatibles et des terres rares, ainsi que les compositions des minéraux, semblent indiquer des événements précoces de fusion partielle affectant à la fois la lherzolite et la harzburgite. L'enrichissement en terres rares légères de la harzburgite, ainsi que le développement de spinelle chromifère et de trémolite, et la distribution des éléments du groupe du platine dans la dunite et la harzburgite, concordent avec l'hypothèse d'une interaction entre magma et peridotite. Le liquide silicaté aurait été de composition boninitique, généré dans la tranche du manteau situé directement par dessus la zone de subduction. La harzburgite s'est formée à un rapport de magma à roche plus faible par rapport à la dunite à cause de l'assimilation partielle de clinopyroxène et d'orthopyroxene de la lherzolite hôte. La dunite se serait formée par assimilation de clinopyroxène et de l'orthopyroxène, et par remplacement du spinelle alumineux par le spinelle chromifère là où le magma boninitique stagnant a réagi avec la lherzolite hôte. Dans la harzburgite et la dunite, la différenciation subséquente du magma a donné des regions à faible teneur en Cr dans les grains de spinelle. L'implication du magma boninitique et une contribution importante de H_2O lors de la formation de la harzburgite et de la dunite, ainsi que l'évidence minéralogique, surtout la présence d'olivine à forte teneur en Fo et Cr dans la

§ *E-mail address*: skaripi@upatras.gr

dunite et d'un spinelle chromifère dans la dunite et la harzburgite, font penser à un milieu de subduction pour l'origine des massifs ophiolitiques de Iti et Kallidromon. De plus, la covariation des rapports Cr/Al et Ni/Al, semblable au cas de la suite ophiolitique bien connue de Vourinos, vient étayer cette hypothèse.

(Traduit par la Rédaction)

Mots-clés: ophiolite, roches ultramafiques, terres rares, éléments du groupe du platine, interaction magma–péridotite, Iti, Kallidromon, Grèce.

Introduction

The Neotethyan ophiolites of Greece outcrop as two main N–S-trending belts. The best-known Greek ophiolite complexes, Vourinos, Pindos and Othrys, belong to the western ophiolitic belt. Harzburgite, with associated dunite, is the dominant ultramafic component of all the western ophiolites, although a few massifs in Othrys are predominantly lherzolitic. The poorly known Iti and Kallidromon ophiolites are located to the south of the Pindos and Othrys ophiolites, and may represent a southward continuation of the western belt.

In this paper, we present new geochemical data (whole-rock and electron microprobe) on ultramafic rocks from the Iti and Kallidromon ophiolite complexes. We aim to investigate the nature and petrogenetic evolution of the upper mantle of that area and the rather unusual spatial association of dunite and lherzolite, as well as to consider the geotectonic setting of the Iti and Kallidromon ophiolites.

Geological Setting

Iti Mountain

Iti Mountain lies to the south of Othrys Mountain and the Sperchios River, in continental central Greece. It belongs to the "Pelagonia terrane" (Stampfli 1996, Stampfli *et al*. 1998), a carbonate platform equivalent to the "Internal carbonate platform" of Papanikolaou (1989). The structure of Iti Mountain is characterized by the superposition of allochthonous units (Beotian, Pelagonian and Ophiolite units) on a basement consisting of rocks belonging to the Pindos and Parnassos isopic zones (Wigniolle 1977). The Iti Mountain (Fig. 1) is composed of five structural units, which from bottom

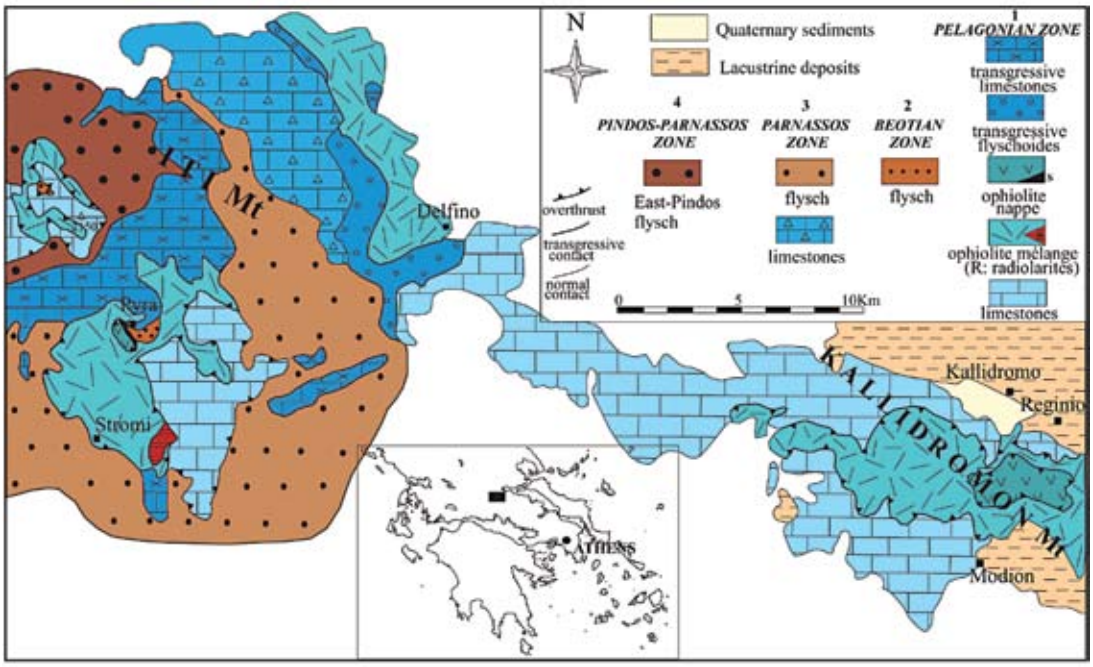

FIG. 1. Simplified geological map of the Iti and Kallidromon Mountains (continental central Greece) (R: radiolarites, S: metamorphic sole).

to top include: the flysch of the East Pindos syncline, Mesozoic platform carbonates along with flysch of the Parnassos zone, the Beotian flysch, the Jurassic platform carbonates of the Pelagonian zone, and the overthrust ophiolite nappe (Celet 1976, Celet *et al*. 1977, Richter *et al*. 1997). The ophiolite is transgressively overlain by Upper Cretaceous formations (Celet 1962, Wigniolle 1977).

Detailed fieldwork has revealed that the Ophiolite Unit is almost entirely represented by an ophiolite mélange; this formation is formerly known as "mélange de type volcano-sédimentaire" (Celet 1976) or "mélange à éléments ophiolitiques" (Celet *et al*. 1977). Remnants of an ophiolite nappe occur to the northwest of Pyra village (southern Iti, see Fig. 1). The ophiolite mélange is comprised of a chaotic and heterogeneous formation that includes rock fragments of varied composition, surrounded by a tectonized matrix. Intense deformation resulted also in fracturing, faulting and shearing occurring throughout the ophiolite mélange, as well as folding of local beds of the pelitic sandstone matrix. The fragments have variable size and include peridotites (both lherzolite and harzburgite), olivine gabbro, gabbro, diorite, dolerite, pillow lava, amphibolite, coarse-grained amphibolite, garnet-bearing amphibolite, radiolarite, sandstone, limestone and scarce listwanite. On the basis of stratigraphic evidence, Celet *et al*. (1977) and Wigniolle (1977) suggested an Upper Jurassic age for this formation, whereas radiolarian age determination (from the radiolarite blocks) implies an Upper Jurassic – Lower Cretaceous age (Baumgartner & Bernoulli 1976, Baumgartner 1984). A remnant ophiolite nappe comprising harzburgite and lherzolite, veined by rare rodingite dykes, is tectonically underlain by an amphibolite sole, at Tsouma Mountain (northwest of Pyra village, see Fig. 1).

Kallidromon Mountain

The Kallidromon Mountain lies to the north of Parnassos Mountain and south of the Maliakos Gulf, in continental central Greece; it belongs geotectonically to the Pelagonian zone (Stampfli 1996, Stampfli *et al*. 1998). The structure of the Kallidromon Mountain (Fig. 1) displays considerable similarities with that of the Iti Mountain, but it is generally less complicated. It is characterized by the presence of the Jurassic Pelagonian platform carbonates and the overthrusted ophiolite (Papastamatiou *et al*. 1962, Celet *et al*. 1977, Leluc 1978, Richter *et al*. 1997). The ophiolite is unconformably overlain by Upper Cretaceous transgressive formations (Celet 1962, Papastamatiou *et al*. 1962).

The Ophiolite Unit is composed of an ophiolite mélange, similar to that described from Iti, and a remnant ophiolite nappe consisting of serpentinized harzburgite and lherzolite; minor dunite forms lensoid bodies, from some dm up to 1 m in size, in the lherzolite. Contacts between the dunite and the adjacent lherzolite may be either sharp or gradational; where dunitic bodies are more tabular with sharp contacts, they resemble intrusive dykes. The whole complex, along with its basement, forms a major synform of WNW–ESE orientation (Fig. 1). Radiolarian age determination suggests a late Middle Jurassic age for the radiolaritic blocks occurring in the ophiolite mélange of Kallidromon (Danelian & Robertson 1995).

Petrography of the Ultramafic Rocks of Iti and Kallidromon

Ultramafic samples were collected from both the ophiolite mélanges and the remnant ophiolite nappes from Iti and Kallidromon. The samples comprise harzburgite, lherzolite and dunite that show variable degrees of serpentinization; where alteration was too intensive, sample nomenclature was based on their normative mineralogy on an anhydrous basis, according to the method of Lensch (1968).

The dunite, collected only from Kallidromon, is the least serpentinized lithology among the studied ultramafic rocks. It displays porphyroclastic to mylonitic textures (Fig. 2a), with olivine (85–90 vol. %), clinopyroxene (1–3 vol.%), disseminated chromian spinel (10–15 vol.%), scarce tremolite and chlorite and rare magnetite grains. Olivine porphyroclasts (2.5–3.5 mm) are usually elongate and exhibit well-developed undulatory extinction and strain lamellae. Intense deformation results locally in a mylonitic texture, where elongate olivine porphyroclastic grains show a preferred orientation and are surrounded by fine-grained recrystallized olivine matrix (Fig. 2a). The clinopyroxene is diopside and occurs as individual granular crystals or pockets of crystals, at olivine triple points, whereas needle-shaped grains of tremolite also occur among olivine grains (Fig. 2b). Moreover, both fine needles of tremolite and granular diopside occur in the tectonized zones of fine-grained olivine (Fig. 2c), traversing the dunite. Subhedral to euhedral crystals of spinel are commonly inhomogeneous, displaying a zoning pattern of Cr-rich to Cr-poor areas, from core to rim of the crystals (Fig. 2d). In some cases the high-Cr compositions extend over almost at the entire crystal. Ferrian chromite or chromian magnetite (Evans & Frost 1975, Barnes 2000, respectively) commonly rims the spinel grains. Alteration of olivine has resulted in the development of serpentine within cracks.

The lherzolite samples have protogranular to porphyroclastic textures (Mercier & Nicolas 1975, Harte 1977). Their modal mineralogy includes olivine (50–70 vol.%), orthopyroxene (15–20 vol.%), clinopyroxene (10–20 vol.%), aluminous spinel (up to 5%) and rare tremolite. They display structures due to plastic deformation such as undulose extinction, strain lamellae, kink bands, rotation, shearing and recrystallization, all typical features of Alpine-type upper mantle peridotites. Olivine forms porphyroclastic grains (<2

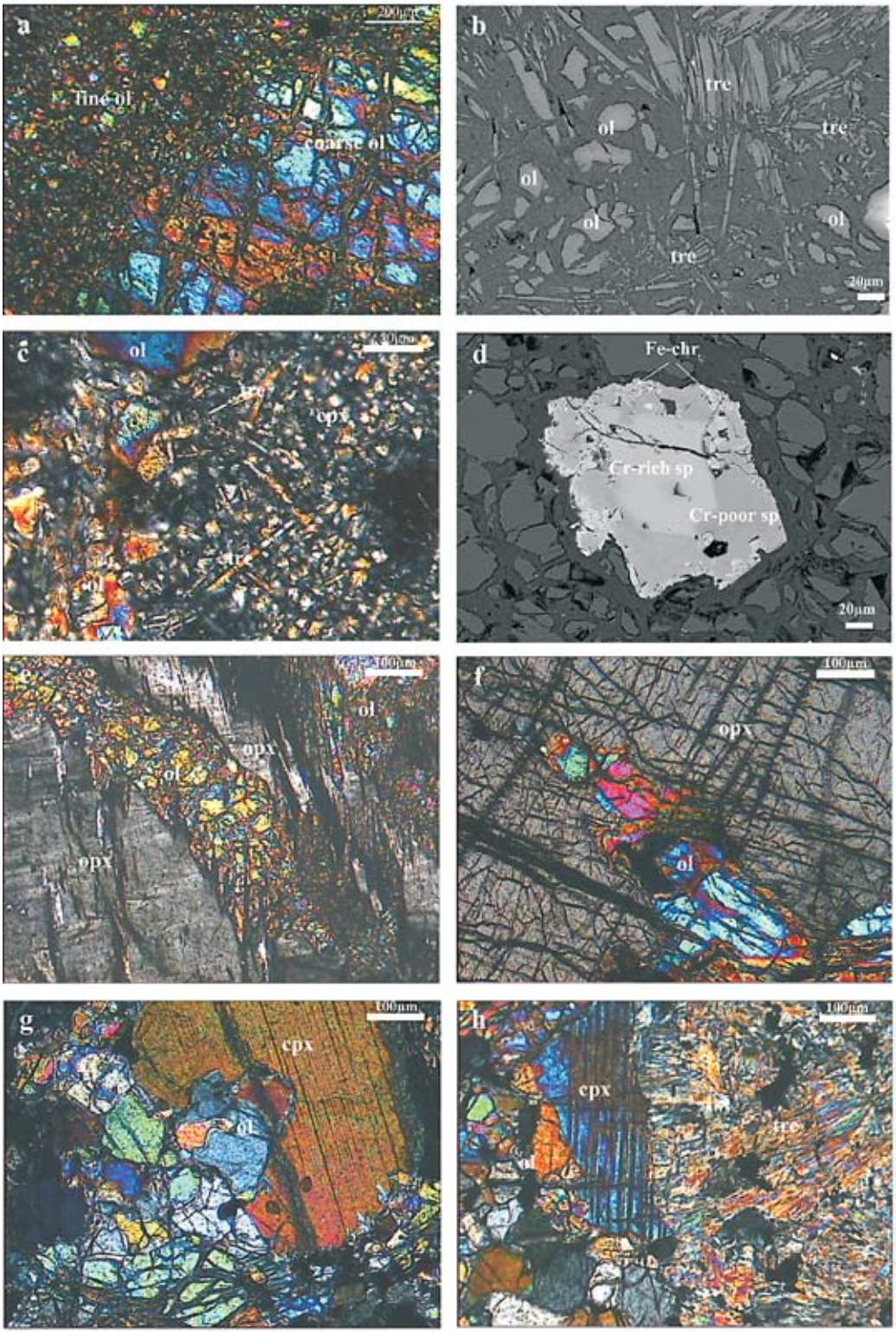
a
fine ol
coarse ol
b
tre
ol
tre
ol
ol
ol
tre
ol
20μm
c
ol
tre
opx
tre
ol
d
Fe-chr
Cr-rich sp
Cr-poor sp
20μm
e
ol
opx
ol
opx
f
opx
ol
g
cpx
ol
h
cpx
tre

mm) with undulatory extinction and deformation twinning, as well as smaller polygonal neoblasts (~0.2 mm) with abundant 120% triple junctions. Olivine neoblasts generally surround porphyroclasts of enstatite (<5 mm) with undulatory extinction. The enstatite commonly has lobate boundaries and shows diopside and augite exsolution lamellae (defined also by electron microscopy), as well as bending, kink bands and gliding parallel to (001). The clinopyroxene is diopside and occurs as neoblastic grains in the recrystallized matrix. Patches of fine- to coarse-grained olivine locally replace orthopyroxene porphyroclasts and clinopyroxene grains (Figs. 2e–g). This replacement is more intensive in samples collected close to the contacts with the dunite. Tremolite forms individual crystals or pockets of needle-shaped crystals (Fig. 2h). The aluminous spinel forms subhedral to anhedral grains with lobate boundaries, usually surrounded and veined by a rim of magnetite. Accessory pentlandite and native copper are dispersed throughout the rocks and are commonly cross-cut by veins of serpentine and Fe-oxides.

The harzburgite samples have been intensively serpentinized. Their assemblage includes mainly serpentine (60–80%), as well as variable percentages of chlorite, actinolite, talc, brucite and calcite; accessory pentlandite, native copper and millerite occur as well. Relict orthopyroxene, clinopyroxene, olivine and chromian spinel (< 20%) also are present. The spinel grains are commonly subhedral to euhedral and show two compositions, usually displaying Cr-rich areas irregularly distributed among Cr-poor ones. Ferrian chromite uncommonly rims the chromian spinel grains; magnetite is more common as a rim and along micrometric fractures. Millerite is typically developed during serpentinization, as Fe decreases and Ni increases in sulfides under such a process (Shiga 1987).

An XRD study revealed that the serpentine polymorphs present in the serpentinized areas of all samples are antigorite and lizardite; these display a variety of textures, such as mesh, hourglass, interpenetrating, interlocking and ribbon (O'Hanley 1996).

FIG. 2.a. Photomicrograph (XPL) of dunite (sample Kl28a) from Kallidromon with porphyroclastic and mylonitic texture, in which flattened porphyroclastic grains of olivine (coarse ol) are surrounded by fine-grained recrystallized olivine matrix (fine ol). b. Back-scatter-electron image (SEM) of dunite (sample Kl21) from Kallidromon showing interstitial needle-shaped tremolitic grains (tre) at olivine (ol) triple points. c. Photomicrograph (XPL) of dunite (sample Kl21) from Kallidromon in which fine needles of tremolite (tre) and granular interstitial clinopyroxene (cpx) occur in the tectonized zones of fine-grained olivine, traversing the dunite. d. Back-scatter-electron image (SEM) of a spinel crystal in dunite displaying a zoning pattern of Cr-rich to Cr-poor areas from core to the rim (sample Kl28a, Kallidromon). The rim of the crystal is replaced by ferrian chromite (Fe–chr). e–f. Photomicrographs (XPL) of lherzolites from Kallidromon (samples Kl46, Kl24) showing fine to coarse olivine grains (ol) replacing orthopyroxene porphyroclasts (opx). g. Photomicrograph (XPL) of lherzolite from Kallidromon (sample Kl46) showing olivine grains (ol) replacing clinopyroxene (cpx). h. Photomicrograph (XPL) of lherzolite from Kallidromon (sample Kl46) in which needle-shaped tremolite (tre) occurs with olivine (ol) and clinopyroxene (cpx).

ANALYTICAL TECHNIQUES

Electron-probe micro-analyses were carried out at the Laboratory of Electron Microscopy and Microanalysis, University of Patras, using a JEOL JSM–6300 SEM, equipped energy-dispersion and wavelength dispersion spectrometers (EDS, WDS) and a THETA software. Operating conditions were accelerating voltage 15 kV and beam current 3.3 nA. Whole-rock chemical analyses were performed at ACTLABS, Ancaster, Ontario, by fusion-ICP for major elements, ICP–MS for trace elements and INAA for rare-earth elements (REE); analyses for the platinum-group elements (PGE) were carried out using preconcentration by NiS fire assay and final determination by INAA. Detection limit for major elements is 0.01%, except for TiO_2 and MnO, for which it is 0.001%. The analytical precision calculated from replicate analyses is better than 3% for most major elements and better than 5% for most trace elements and the REE. A precision better than 15% was achieved for the PGE.

MINERAL COMPOSITIONS

Spinel-group minerals

Representative compositions of the spinel-group minerals from the Iti and Kallidromon peridotites are given in Table 1. The lherzolite contains Cr-poor, Al-rich spinels, with Cr# [molar 100 × Cr/(Cr + Al)] ranging from 13.8 to 32.3 (Table 1). The Kallidromon dunite commonly contains two compositional varieties of chromian spinel (Fig. 3), even in the same crystal. Where the chromian spinel grains are inhomogeneous, they display a zoning pattern characterized by depletion of Cr and enrichment in Mg, from core to the rim (Fig. 2d, anal. Kl28a/14c and Kl28a/14r, in Table 1). The Cr-rich core composition has Cr# in the range 83.1–87.1; the analyzed spots, on a Cr# *versus* Mg# diagram, form a cluster at the low-Mg# end of the diagram (Fig. 3). The rim composition of chromian spinel is poorer in Cr, with Cr# in the range of 60.4 to 75.6, and richer in Mg, showing linear covariation with Mg# (Fig. 3). The composition of the Cr-rich spinels in harzburgitic rocks also is variable, as was mentioned earlier, but in comparison to the dunitic ones they are slightly poorer in Cr (Table 1, Fig. 3). The Cr-poor compositional areas have 43.8 < Cr# < 55.8, showing a linear covariation with Mg#, whereas those richer in Cr have 80.4 < Cr#

< 83.0. The Cr-rich spinel in harzburgitic rocks plots close to the Cr-rich spinel compositions in the dunitic rocks, but at lower Mg# values (Fig. 3).

The Cr# in spinel can be regarded as a sensitive chemical parameter for the degree of depletion as long as it lies above 15 (Dick & Bullen 1984). The Cr# in spinel is also a good indicator of the tectonomagmatic history of the host rock. The Cr-poor spinel grains in lherzolitic and harzburgitic rocks display a low Cr# (<60) typical of oceanic ophiolites (including back-arc basins) whereas, in arc-related ophiolitic sequences, spinel grains have a Cr# greater than 60 (Dick & Bullen 1984). The grains of Cr-poor spinel from the harzburgite show a rather broad range and are similar in terms of Cr# to spinel from Alpine-type peridotites, but at a lower Mg#. The grains of Al-rich spinel from the lherzolite are analogous to those from abyssal peridotites (Fig. 3). Both the spinels in dunite and the Cr-rich spinel in harzburgite plot at higher Cr# values (analogous to those from both Alpine type and arc-related peridotites), but possess slightly lower Mg# values than those from the Alpine type peridotites (Fig. 3).

The ferrian chromite rims plot at the high-Cr#, low-Mg# end of the diagram (Fig. 3). Their occurrence has been assigned to oxidation of Fe^{2+} and contemporaneous dissolution of Al (McInnes *et al.* 2001). Formation of secondary magnetite after Cr-rich spinel is in line with this interpretation. The formation of ferrian chromite and magnetite is broadly assigned to prograde metamorphism of Cr-rich spinel (*e.g.,* Bliss & MacLean 1975, Roeder 1994, Abzalov 1998, Barnes 2000). Their detailed investigation is beyond the scope of this study.

The considerable differences among the spinel compositions can best be illustrated with the plot of Cr# in spinel *versus* Fo content in olivine (Fig. 4). The spinel–olivine pairs in the lherzolitic, harzburgitic, and most of the dunitic rocks plot within the OSMA (olivine–spinel mantle array; after Arai 1994a). The pairs in lherzolites plot in the abyssal peridotite field, although this is not diagnostic, as peridotites from passive margins, oceanic arcs and marginal basins may also plot in this field. The chromian spinel – olivine pairs from the dunitic and harzburgitic samples are consistent with a supra-subduction zone (SSZ) origin (Dick & Bullen 1984, Bonatti & Michael 1989, Arai 1994a). The Cr-rich spinel – olivine pairs from the dunite lie within or near the olivine–spinel mantle array (Fig. 4). The lherzolites plot close to the fertile mantle composition (FMM), consistent with their more primary nature.

Zhou *et al.* (1996, 1998, 2005) showed that high-Cr chromites in the Luobusa ophiolite crystallized from suprasubduction-zone boninitic melts. The Cr-rich spinel – olivine pairs from the dunite sample studied, shown in Figure 4, follow the trend defined by the fractionation line of boninites (Arai 1994b). According to Arai (1994b), boninites contain a spinel with a high Cr# (around 90) and olivine with a high Fo, that lies within or near the olivine–spinel mantle array. The Fo–Cr# fractionation lines reflect the differentiation of magma including various processes such as crystallization differentiation, magma mixing and assimilation. Besides, the observed depletion in Cr in the spinels from dunites from core to the rim of the crystal is a common feature of Cr-rich spinel crystallized from melt (Leblanc & Ceuleneer 1992).

Pyroxenes

Representative results of pyroxene micro-analyses from the Iti and Kallidromon ultramafic rocks are

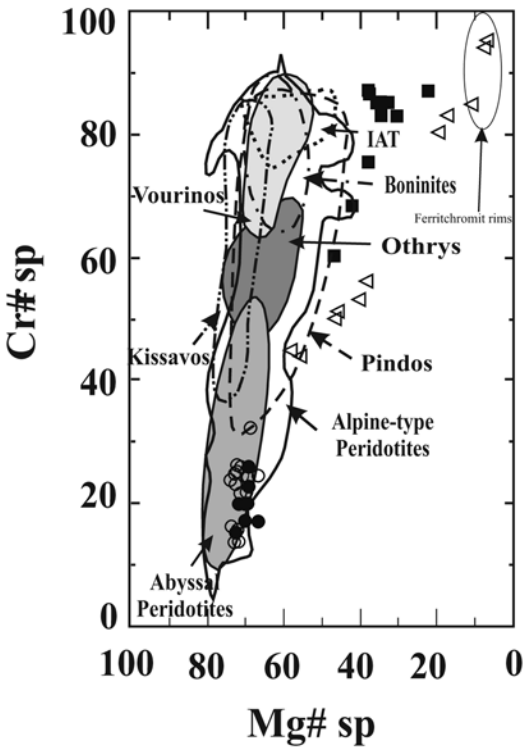

FIG. 3. Spinel compositions from the Iti and Kallidromon peridotites, in terms of Cr# [100 Cr/(Cr+Al)] against Mg# [100Mg/(Mg+Fe^{2+})] ratio. Fields for spinels occurring in Alpine-type peridotites, abyssal peridotites, Tertiary boninites from the Western Pacific and Cape Vogel, Papua and island-arc rocks from Troodos, Othrys and Aegina (Greece), are shown for comparison (Dick & Bryan 1979, Dick & Bullen 1984, Cameron *et al.* 1979, Dietrich *et al.* 1987). Also shown the fields from Pindos, Vourinos, Kissavos and Othrys (data after Economou-Eliopoulos *et al.* 1999, Economou-Eliopoulos & Vacondios 1995). Symbols: ○ Iti lherzolites, ● Kallidromon lherzolites, Δ Iti harzburgites, ■ Kallidromon dunites.

listed in Table 2. The ferric iron content was calculated according to the method of Papike *et al*. (1974). All the analyzed pyroxenes are chemically homogeneous, with no distinctive zoning, consistent with subsolidus re-equilibration. According to the I.M.A. classification (Morimoto *et al*. 1988), the orthopyroxene of the harzburgites and lherzolites is enstatite (Table 2). Its Al content decreases from the lherzolite to the harzburgite, whereas Ca and Mg contents generally increase toward that of the enstatite in harzburgite (Table 2). Exsolution lamellae of augite and diopside have been observed in the orthopyroxenes. The clinopyroxene of the ultramafic samples is diopside. Clinopyroxene porphyroclasts in the lherzolite have low Na and Ti contents, similar to clinopyroxenes from abyssal peridotites (Dick 1989, Johnson *et al*. 1990). The analyzed diopside from harzburgite is poorer in Al and Cr and richer in Mg, Ca and Na contents, relative to that from lherzolitic rocks. The analyzed diopside from the dunite has lower Al and Fe and higher Si contents relative to the diopside in harzburgite. The diopside in lherzolite is poorer in Mg relative to that in harzburgitic and dunitic rocks (Table 2).

Olivine

Representative results of olivine micro-analyses from the Iti and Kallidromon ultramafic rocks are given in Table 3. Both the porphyroclastic and neoblastic analyzed grains in the lherzolite and harzburgite are compositionally similar and homogeneous. The Fo content [100 × Mg/(Mg + Fe^{2+}), molar] in olivine decreases slightly from the dunite ($Fo_{.90}$–$Fo_{.93}$) to the harzburgite ($Fo_{.86–.90}$) and the lherzolite ($Fo_{.87}$–$Fo_{.91}$). The Fo content in some of the harzburgitic rocks is lower than that expected from typical harzburgites, most probably due to Mg loss during serpentinization (*e.g.*, O'Hanley 1996, Melcher *et al*. 2002). The Fo values of the olivine grains are mostly comparable to those of peridoties from oceanic ridgez and supra-subduc-

TABLE 1. REPRESENTATIVE COMPOSITIONS OF SPINEL FROM THE ULTRAMAFIC ROCKS OF ITI (I) AND KALLIDROMON (KL)

	Lherzolites								Harzburgites							Dunites			
Sample	I30 /25	I30 /32	I617 /1	I617 /2	Kl24a /2	Kl24a /25	I290 /3	I290 /13	Kl17 /22	Kl17 /32	I455 /19c	I455 /20r	I476 /5c	I476 /5i	I476 /5r	Kl21 /6	Kl21 /9	Kl28a /14c	Kl28a /14r
SiO_2	-	-	-	-	0.04	0.25	0.33	0.37	-	-	-	-	-	-	-	-	-	0.23	0.08
TiO_2	0.06	0.05	-	-	-	0.06	-	-	0.09	0.08	-	-	-	-	-	-	0.17	0.17	0.22
Al_2O_3	46.85	44.84	40.63	45.29	49.54	51.49	54.89	54.84	30.22	30.70	22.87	4.39	8.58	6.67	1.40	8.34	7.22	6.92	15.30
Cr_2O_3	20.76	23.76	28.93	23.70	18.11	15.71	13.15	13.09	36.44	35.71	43.05	36.57	52.42	48.58	34.86	61.00	62.06	59.78	49.76
FeO'	13.51	13.40	13.98	13.65	13.59	14.14	12.50	12.78	18.77	19.61	25.51	56.73	34.45	40.39	60.82	23.85	23.96	26.40	25.00
MnO	0.12	0.15	-	-	0.35	0.37	-	0.05	0.28	0.32	-	-	0.60	0.61	1.19	-	0.18	-	0.53
MgO	17.89	17.82	16.43	17.53	16.76	17.17	18.28	17.86	12.87	12.20	8.12	2.29	3.72	3.45	1.50	5.88	6.86	6.49	8.78
CaO	0.03	0.01	-	-	0.09	-	-	-	0.05	-	-	-	-	-	-	-	-	-	0.14
Na_2O	0.05	0.01	-	-	-	-	-	-	-	-	-	-	-	-	-	-	-	-	-
K_2O	-	0.01	-	-	0.02	-	-	-	-	0.01	-	-	-	-	-	0.15	0.05	-	-
NiO	-	-	-	-	0.19	0.50	0.55	0.40	0.10	0.13	-	-	-	-	-	-	-	-	-
Total	99.27	100.05	99.97	100.17	98.69	99.69	99.70	99.39	98.82	98.76	99.55	99.98	99.77	99.70	99.77	99.22	100.50	99.99	99.81
Si	-	-	-	-	0.009	0.054	0.070	0.078	-	-	-	-	-	-	-	-	-	0.064	0.021
Al	12.118	11.617	10.758	11.711	12.782	13.075	13.657	13.695	8.625	8.783	6.899	1.622	2.882	2.310	0.539	2.712	2.324	2.256	4.760
Cr	3.601	4.128	5.136	4.110	3.133	2.675	2.194	2.192	6.974	6.851	8.708	9.062	11.807	11.280	8.997	13.302	13.397	13.069	10.380
Ti	0.010	0.008	-	-	-	0.010	-	-	0.016	0.015	-	-	-	-	-	-	0.035	0.035	0.044
Fe^{3+}	0.271	0.247	0.106	0.179	0.076	0.186	0.079	0.035	0.385	0.351	0.393	5.316	1.311	2.410	6.464		0.244	0.576	0.795
Σ	16.000	16.000	16.000	16.000	16.000	16.000	16.000	16.000	16.000	16.000	16.000	16.000	16.000	16.000	16.000	16.014	16.000	16.000	16.000
Mg	5.857	5.844	5.507	5.738	5.474	5.519	5.758	5.646	4.650	4.419	3.101	1.071	1.582	1.512	0.731	2.421	2.796	2.678	3.457
Fe^{2+}	2.210	2.218	2.523	2.328	2.414	2.364	2.130	2.231	3.419	3.633	5.072	9.571	6.906	7.521	10.158	5.508	5.234	5.536	4.728
Mn	0.022	0.028	-	-	0.065	0.068	-	0.009	0.057	0.066	-	-	0.145	0.152	0.329	-	0.042	-	0.119
Ca	0.007	0.002	-	-	0.021	-	-	-	0.013	0.000	-	-	-	-	-	-	-	-	0.040
Ni	-	-	-	-	0.034	0.087	0.094	0.068	0.020	0.025	-	-	-	-	-	-	-	-	-
ΣCat.	24.096	24.092	24.030	24.066	24.008	24.038	23.982	23.954	24.159	24.143	24.173	26.642	24.633	25.185	27.218	23.943	24.072	24.214	24.344
Cr#	22.92	26.23	32.33	25.99	19.70	16.99	13.85	13.81	44.73	43.84	55.81	84.83	80.39	83.01	94.35	83.07	85.22	85.29	68.58
Mg#	70.24	70.33	67.69	69.60	68.73	68.40	72.27	71.35	55.00	52.58	36.20	6.71	16.14	13.21	4.21	30.53	33.79	30.47	38.50

The compositions are reported in weight %, then are recast as structural formulae, in atoms per formula unit (*apfu*) on the basis of 32 atoms of oxygen. Symbols: c: core, i: intermediate, r: rim. Cr# = 100[Cr/(Cr + Al)], Mg# = 100[Mg/(Mg + Fe^{2+})]. -: Concentration below detection limit.

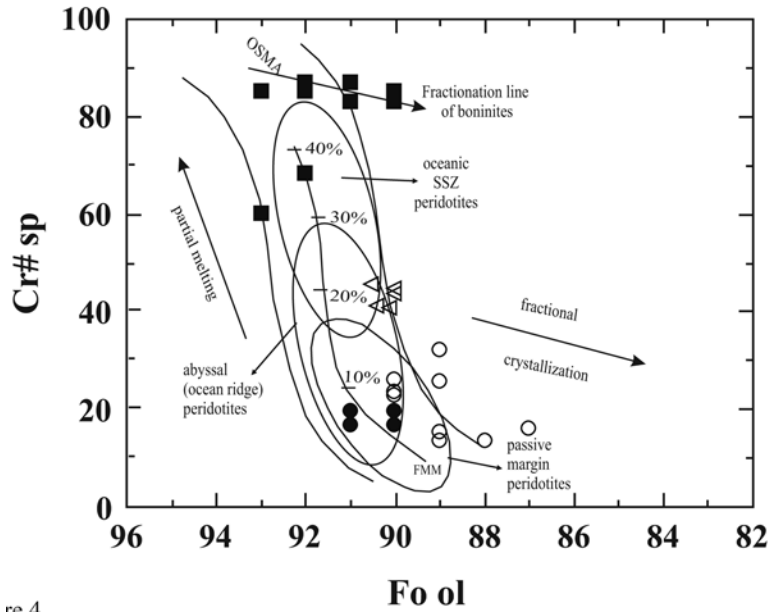

FIG. 4. Cr# in spinel *versus* Fo content of olivine in ultramafic rocks from Iti and Kallidromon. Fields for spinels occuring in abyssal (ocean-ridge) peridotites, oceanic SSZ peridotites and passive-margin peridotites are after Dick & Bullen (1984) and Pearce *et al*. (2000). OSMA field and fractionation line of boninites are after Arai (1994a, b), respectively.

tion zones (Arai 1994a). NiO contents are rather low compared to olivine from Alpine peridotites.

Amphibole

Representative compositions of amphibole from the lherzolite and dunite from Iti and Kallidromon are listed in Table 4. According to the classification of Leake *et al*. (1997), the amphibole is tremolite. In dunite, the tremolite has lower Al, Fe, Mn, and Na contents and higher Mg contents than lherzolite (Table 4). The grains are commonly inhomogeneous without displaying typical zoning. These compositional heterogeneties are due to variation mainly of Ca, Al and Mg contents in the same crystal.

WHOLE-ROCK CHEMISTRY

Results of whole-rock chemical analyses of ultramafic rocks from Iti and Kallidromon are shown in Table 5. All samples are typically rich in Mg, Cr and Ni, and generally poor in trace elements. The harzburgites are strongly depleted in incompatible major elements (0.03–0.16% CaO, 0.34–1.25% Al_2O_3 and 0.04–0.45% Na_2O) relative to the average primitive upper mantle (PUM; 3.2–3.6% CaO, 4.0–4.5% Al_2O_3, 0.33–0.61 Na_2O; *e.g*., Bonatti & Michael 1989, Allègre *et al*. 1995), suggesting a highly refractory nature. The lherzolites, although richer in these major elements than the harzburgites, also show lower abundances relative to PUM. The TiO_2 contents in all but two samples (Kl 19 and Kl 24) are lower than that of mid-ocean-ridge mantle rocks (0.1–0.4 %) and consistent with that from mantle rocks formed in a supra-subduction zone (SSZ) environment (<0.1; Pearce *et al*. 1984). The Mg# values vary between 81.2 and 83.4 in the harzburgites, between 80.1 and 85.2 in the lherzolites and between 85.1 and 87.2 in the dunites (Table 5); all these values are lower than Mg# in average primitive upper mantle (89.8). The harzburgites have CaO/Al_2O_3 ratios much lower than PUM (0.8). In contrast, the lherzolites display higher CaO/Al_2O_3 ratios, analogous to PUM (Table 5). The dunites are poorer in Al than the harzburgites, resulting in much higher CaO/Al_2O_3 ratios (Table 5). Their CaO content is higher than that expected for ordinary dunites owing to the presence of minor clinopyroxene and tremolite. The harzburgites have also higher Ni and lower V abundances relative to the lherzolites; Ni contents in both lithotypes (1890 ppm) are higher than PUM whereas the amount of V is lower than PUM (82 ppm; values from McDonough & Sun 1995). Concentrations of Ni increase and of Cu decrease from the lherzolites through the harzburgites to the dunites (Table 5).

TABLE 2. REPRESENTATIVE COMPOSITIONS OF PYROXENE FROM ULTRAMAFIC ROCKS OF ITI (I) AND KALLIDROMON (KL)

	Lherzolites											Harzburgites							Dunites		
	En		Di		En		Di		En		Di	En		Di		En		Di	Di		
Sample	I	I	I	I	Kl	Kl	Kl	Kl	I	I	I	I	I	I	I	Kl	Kl	Kl	Kl	Kl	Kl
	617	617	617	617	24a	24a	24a	24a	289	289	289	264	264	264	264	17	17	17	21	28a	28a
	25pc	27pc	18	26	14	15	26	27	1	10	4n	21	21d	19	25	26	29	16	4	4	5
SiO_2 wt%	57.19	55.54	53.18	52.97	54.71	53.79	53.9	52.89	55.16	55.94	52.46	55.83	55.94	53.93	53.15	55.12	55.51	52.75	56.00	55.00	55.31
TiO_2	-	-	0.26	0.29	0.05	0.07	0.38	0.30	-	-	0.14	0.06	0.04	0.05	0.09	-	-	0.36	-	-	-
Al_2O_3	2.44	3.94	3.81	4.10	5.48	4.87	3.88	4.72	4.78	5.35	4.26	2.35	1.95	0.97	1.76	4.53	3.99	2.48	0.46	0.63	0.49
Cr_2O_3	-	0.91	0.82	0.97	0.59	0.71	0.63	0.62	0.57	0.76	0.63	0.60	0.55	0.32	0.56	0.99	0.90	0.71	0.32	0.27	0.39
FeO'	7.08	7.21	2.38	2.31	6.48	6.02	2.23	2.34	7.03	7.32	2.68	6.45	6.87	2.00	2.44	7.35	6.94	2.84	1.09	1.45	1.73
MgO	32.58	31.59	16.62	16.31	31.27	32.56	16.36	16.26	30.04	30.11	14.75	32.94	33.27	17.65	17.29	30.77	31.20	15.86	17.51	18.19	17.83
NiO	-	-	-	-	0.21	-	-	-	0.12	-	0.17	0.13	0.09	-	0.01	-	-	0.25	0.10	-	-
MnO	-	-	0.05	0.07	0.02	0.33	0.37	0.27	0.08	-	-	0.13	0.08	0.03	0.09	0.27	-	-	-	-	-
CaO	0.73	1.06	22.68	22.85	0.45	0.80	23.16	22.67	2.04	1.05	24.62	1.30	1.11	24.84	23.86	0.56	1.95	24.74	24.53	24.17	24.26
Na_2O	-	-	0.88	0.76	-	-	-	-	-	-	-	0.04	0.05	0.11	0.24	-	-	-	-	-	-
K_2O	-	-	-	0.01	-	-	-	-	0.10	-	-	-	0.01	0.01	-	-	0.11	-	-	-	-
Total	100.02	100.25	100.68	100.64	99.26	99.15	100.91	100.07	99.92	100.53	99.71	99.83	99.96	99.91	99.49	99.59	100.60	99.99	100.01	99.71	100.21
Si	1.983	1.929	1.911	1.908	1.913	1.873	1.949	1.925	1.929	1.946	1.928	1.937	1.938	1.957	1.939	1.933	1.923	1.932	2.033	1.997	2.007
^{IV}Al	0.017	0.071	0.089	0.092	0.087	0.127	0.051	0.075	0.071	0.054	0.072	0.063	0.062	0.041	0.061	0.067	0.077	0.068	-	0.003	-
Σ	2.000	2.000	2.000	2.000	2.000	2.000	2.000	2.000	2.000	2.000	2.000	2.000	2.000	2.000	2.000	2.000	2.000	2.000	2.033	2.000	2.007
^{VI}Al	0.083	0.090	0.072	0.082	0.139	0.073	0.114	0.128	0.126	0.165	0.113	0.033	0.017	-	0.014	0.120	0.086	0.039	0.020	0.024	0.021
Ti	-	-	0.007	0.008	0.001	0.002	0.010	0.008	-	-	0.004	0.002	0.001	0.001	0.002	-	-	0.010	-	-	-
Fe^{3+}	-	-	0.041	0.020	-	0.030	-	-	-	-	-	0.013	0.032	0.039	0.043	-	-	-	-	-	-
Fe^{2+}	0.205	0.209	0.031	0.050	0.190	0.146	0.067	0.071	0.206	0.213	0.082	0.174	0.167	0.021	0.032	0.216	0.201	0.087	0.034	0.044	0.052
Cr	-	0.025	0.023	0.028	0.016	0.020	0.018	0.018	0.016	0.021	0.018	0.016	0.015	0.009	0.016	0.027	0.025	0.021	0.009	0.008	0.011
Mg	1.685	1.636	0.890	0.876	1.630	1.691	0.882	0.882	1.566	1.562	0.808	1.703	1.718	0.955	0.940	1.608	1.612	0.866	0.948	0.985	0.965
Ni	-	-	-	-	0.006	-	-	-	0.003	-	0.005	0.004	0.003	-	-	-	-	0.007	0.003	-	-
Mn	-	-	0.002	0.002	0.001	0.010	0.011	0.008	0.002	-	-	0.004	0.002	0.001	0.003	0.008	-	-	-	-	-
Ca	0.027	0.039	0.873	0.882	0.017	0.030	0.897	0.884	0.076	0.039	0.970	0.048	0.041	0.966	0.932	0.021	0.072	0.971	0.954	0.940	0.943
Na	-	-	0.061	0.053	-	-	-	-	-	-	-	0.003	0.003	0.008	0.017	-	-	-	-	-	-
K	-	-	-	-	-	-	-	-	0.004	-	-	-	-	-	-	-	0.005	-	-	-	-
Σ	2.000	2.000	2.000	2.000	2.000	2.000	2.000	2.000	2.000	2.000	2.000	2.000	2.000	2.000	2.000	2.000	2.000	2.000	1.968	2.000	1.992
Mg#	89.15	88.67	92.52	92.60	89.56	90.57	92.94	92.55	88.37	88.00	90.79	90.11	89.62	94.09	92.61	88.16	88.91	90.87	96.54	95.72	94.89
Wo %	1.4	2.1	47.5	48.2	0.9	1.6	48.3	47.9	4.1	2.2	52.1	2.5	2.1	48.7	47.8	1.1	3.8	50.5	49.3	47.8	48.1
En	87.9	86.8	48.5	47.9	88.7	88.7	47.5	47.8	84.6	86.1	43.4	87.7	87.6	48.2	48.2	86.8	85.5	45.0	49.0	50.0	49.2
Fs	10.7	11.1	4.0	3.9	10.3	9.7	4.2	4.3	11.2	11.7	4.4	9.8	10.3	3.1	4.0	12.1	10.7	4.5	1.7	2.2	2.7

En: enstatite, Di: diopside, pc: porphyroclast, n: neoblast. -: Concentration below detection limit. The structural formulae are calculated on the basis of six atoms of oxygen.

Figure 5 illustrates the variation of CaO, Al_2O_3, V and Ni against MgO for the ultramafic rocks of Iti and Kallidromon. The peridotites show an inverse correlation of CaO, Al_2O_3 and V with MgO, whereas the Ni displays a positive correlation. Although the correlations of CaO and Al_2O_3 are poor, the defined trends for the above oxides are similar to those of Alpine peridotites.

The ultramafic rocks display generally low REE contents (Table 6), analogous to those of Alpine-type peridotites (*e.g.*, Frey 1984, Johnson *et al*. 1990). The dunites are extremely poor in REE, which are generally below detection limits. The lherzolites have "spoon-shaped" chondrite-normalized REE patterns with an overall depletion in LREE [$0.8 < (Ce/Yb)_N < 0.17$) and relatively unfractionated middle and heavy REE profiles (Fig. 6). Similar patterns have been described for clinopyroxene-rich harzburgites from the Luobusa (Zhou *et al*. 2005) and the Oman ophiolites (Godard *et al*. 2000). The Iti lherzolite is richer in MREE and HREE relative to that from Kallidromon. The harzburgites have a "U-shaped" REE pattern, typical of interaction between LREE-enriched melt and LREE-depleted mantle residues (Fig. 6). We do not understand the reason why Lu in the harzburgites is slightly higher than in the lherzolites. Analogous REE patterns have been described for

TABLE 3. REPRESENTATIVE COMPOSITIONS OF OLIVINE FROM ULTRAMAFIC ROCKS OF ITI (I) AND KALLIDROMON (KL)

	Lherzolites							Harzburgites			Dunites			
Sample	I30 /21	I617 /20n	I617 /26n	Kl24a /7	Kl24a /29	I289 /8	I289 /14	I264 /24	Kl17 /13	Kl17 /33	Kl21 /2	Kl21 /12	Kl28a /19	Kl28a /24
SiO_2	41.38	40.68	41.07	41.56	40.16	40.49	40.74	40.72	40.32	40.13	41.00	40.73	41.22	41.17
Al_2O_3	-	-	-	-	-	-	-	-	-	-	-	-	0.20	0.02
FeO'	9.72	10.56	9.84	9.27	9.25	10.22	10.21	9.55	11.27	13.27	9.00	9.84	7.30	7.92
MnO	0.13	-	-	0.13	0.28	-	0.20	0.23	-	-	0.33	-	-	-
MgO	49.65	48.33	49.29	49.77	49.09	48.33	48.66	49.02	47.99	45.93	49.41	49.15	50.82	50.66
CaO	0.05	-	-	-	-	-	0.12	0.01	-	-	0.03	-	0.13	0.12
Na_2O	-	-	-	-	-	-	-	0.04	-	-	-	-	-	-
K_2O	0.01	-	-	-	-	-	-	-	-	-	-	0.03	-	-
Cr_2O_3	0.02	-	-	-	-	-	-	-	-	-	0.02	-	0.07	0.10
NiO	-	-	-	0.20	0.19	0.51	0.60	0.32	-	0.31	-	-	0.27	-
Total	100.96	99.57	100.20	100.93	98.97	99.55	100.53	99.89	99.58	99.64	99.79	99.75	100.01	99.99
Si	1.003	1.003	1.003	1.005	0.993	1.000	0.998	0.999	0.998	1.003	1.003	0.999	0.999	0.999
Al	-	-	-	-	-	-	-	-	-	-	-	-	0.006	0.001
Mg	1.793	1.776	1.794	1.795	1.810	1.779	1.776	1.793	1.771	1.711	1.802	1.797	1.836	1.833
Fe^{2+}	0.197	0.218	0.201	0.188	0.191	0.211	0.209	0.196	0.233	0.277	0.184	0.202	0.148	0.161
Mn	0.003	-	-	0.003	0.006	-	0.004	0.005	-	-	0.007	-	-	-
Ca	0.001	-	-	-	-	-	0.003	-	-	-	0.001	-	0.003	0.003
Σ	1.994	1.994	1.995	1.986	2.007	1.990	1.992	1.994	2.004	1.988	1.994	1.999	1.993	1.998
ΣCat.	2.997	2.997	2.998	2.991	3.000	2.990	2.990	2.993	3.002	2.991	2.997	2.998	2.992	2.997
Fo	0.90	0.89	0.90	0.91	0.90	0.89	0.89	0.90	0.88	0.86	0.91	0.90	0.93	0.92
Fa	0.10	0.11	0.10	0.09	0.10	0.11	0.11	0.10	0.12	0.14	0.09	0.10	0.07	0.08

The compositions are reported in weight %, then are recast as structural formulae, in atoms per formula unit (*apfu*) on the basis of four atoms of oxygen. N: neoblasts; all other compositions from porphyroclasts. -: concentration below detection limit.

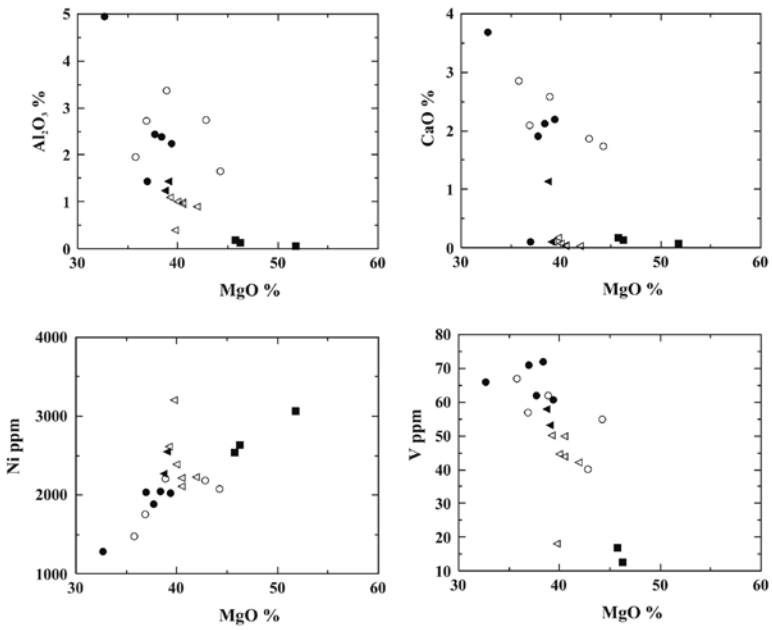

FIG. 5. Variation diagrams of selected elements *versus* MgO content on an anhydrous basis, for ultramafic rocks from Iti and Kallidromon. Symbols: as in Figure 3 except ▲ Kallidromon harzburgites.

harzburgites and dunites of metasomatic origin, from the Luobusa ophiolite (Zhou *et al*. 2005).

Figure 7 illustrates chondrite-normalized PGE patterns. The ultramafic rocks from Iti and Kallidromon display generally smooth PGE patterns with some selective Au-enrichment. The lherzolites are generally richer in PGE (except Os) relative to the harzburgites. The dunites and the lherzolites have higher Pt abundances relative to the harzburgites. Both the harzburgites and dunites show also Ru depletion (with one exception, sample Kl 25 of the dunites). Sample I 317 (harzburgite) has an anomalous PGE pattern, mainly due to Ir, Rh and Pt depletions, and Pd-enrichment. Replicate analyses preclude the involvement of analytical error. The Pd/Ir values (Table 7) range from 1.00 to 2.67 in the analyzed samples, except for sample I 317, with Pd/Ir = 78.

TABLE 4. REPRESENTATIVE COMPOSITIONS OF TREMOLITE FROM LHERZOLITES AND DUNITES OF ITI (I) AND KALLIDROMON (KL)

	Lherzolites			Dunites							
Sample	I289 /15	I289 /16	I289 /17	Kl21 /3a	Kl21 /3b	Kl21 /3c	Kl21 /7	Kl21 /12a	Kl21 /12b	Kl21 /14	Kl21 /15
SiO_2 wt%	57.97	57.77	57.82	57.97	57.93	57.53	58.10	58.68	59.24	58.66	58.53
TiO_2	0.02	0.02	0.01	-	-	-	-	-	-	0.08	-
Al_2O_3	1.36	1.40	1.35	1.49	1.19	0.87	1.04	1.30	1.24	1.00	1.00
Cr_2O_3	0.22	0.25	0.18	0.36	0.23	0.13	-	0.42	0.29	-	0.08
FeO^t	3.21	3.10	3.30	1.64	1.31	1.98	1.76	1.73	1.45	1.31	1.58
MnO	0.10	0.09	0.09	-	-	-	-	-	0.06	0.04	-
MgO	22.27	22.25	22.15	23.87	24.16	24.43	23.85	23.30	24.25	23.48	24.24
CaO	12.93	12.95	12.80	11.49	12.03	12.32	11.79	13.06	11.99	13.33	11.94
Na_2O	0.09	0.07	0.07	-	-	-	-	-	-	0.04	-
K_2O	-	-	-	-	-	-	-	-	-	-	-
NiO	-	-	-	-	-	-	0.16	-	-	-	-
Total	98.17	97.90	97.77	96.82	96.85	97.26	96.70	98.49	98.52	97.94	97.37
Si *apfu*	7.922	7.915	7.938	7.957	7.935	7.850	7.997	7.950	7.992	7.971	7.980
^{IV}Al	0.078	0.085	0.062	0.043	0.065	0.150	0.003	0.050	0.008	0.029	0.020
Σ	8.000	8.000	8.000	8.000	8.000	8.000	8.000	8.000	8.000	8.000	8.000
^{VI}Al	0.141	0.141	0.156	0.198	0.126	-	0.165	0.157	0.189	0.131	0.140
Ti	0.002	0.002	0.001	-	-	-	-	-	-	0.008	-
Cr	0.024	0.027	0.020	0.039	0.025	0.014	-	0.045	0.031	-	0.009
Fe^{3+}	-	-	-	-	-	0.136	-	-	-	-	-
Fe^{2+}	0.296	0.285	0.291	-	-	-	-	0.092	-	0.105	-
Mg	4.537	4.545	4.533	4.763	4.849	4.850	4.835	4.706	4.780	4.756	4.851
Ni	-	-	-	-	-	-	-	-	-	-	-
Mn	-	-	-	-	-	-	-	-	-	-	-
Ca	-	-	-	-	-	-	-	-	-	-	-
Σ	5.000	5.000	5.001	5.000	5.000	5.000	5.000	5.000	5.000	5.000	5.000
Mg	-	-	-	0.122	0.085	0.120	0.059	-	0.097	-	0.076
Fe^{2+}	0.071	0.070	0.088	0.188	0.150	0.079	0.203	0.104	0.164	0.044	0.180
Mn	0.012	0.010	0.010	-	-	-	-	-	0.007	0.005	-
Ca	1.893	1.901	1.883	1.690	1.765	1.801	1.739	1.896	1.733	1.941	1.744
Na	0.024	0.019	0.019	-	-	-	-	-	-	0.011	-
Σ	2.000	2.000	2.000	2.000	2.000	2.000	2.001	2.000	2.001	2.001	2.000
ΣCat.	15.000	15.000	15.001	15.000	15.000	15.000	15.001	15.000	15.001	15.001	15.000

a, b, c: analyzed spots in the same crystal. -: Concentration below detection limit. The structural formulae are calculated on the basis of 23 atoms of oxygen.

Petrogenetic Evolution

Alteration and element mobility

Loss on ignition (LOI) is broadly considered to be a measure of the degree of serpentinization (serpentine minerals contain between 12 and 15 wt. % H_2O; Deer *et al*. 1992). The lherzolites display generally lower LOI values than the harzburgites which are almost entirely serpentinized (Table 5). The LOI of the samples correlates well with the degree of alteration determined petrographically. The mobility of Ca is evaluated with the diagram MgO *versus* MgO/CaO (Fig. 8), in which two groups are distinguished. In the lherzolites, covariation of Mg and Ca is observed at lower MgO/CaO values relative to the harzburgites and dunites. Levels of Mg and Ca, moreover, show no correlation with LOI for the lherzolites (not shown), suggesting their stable behavior during alteration. The harzburgites plot at higher MgO/CaO values and show considerable scatter from *ca*. 100 to 2000. Their CaO content correlates negatively with LOI (not shown), indicating that Ca was removed during serpentinization. The dunites form a trend analogous to the lherzolites at higher MgO/CaO values (Fig. 8).

The Pr_N/Sm_N ratios of the peridotites show no trend with LOI, indicating that serpentinization alone does not govern their LREE variation (Fig. 9).

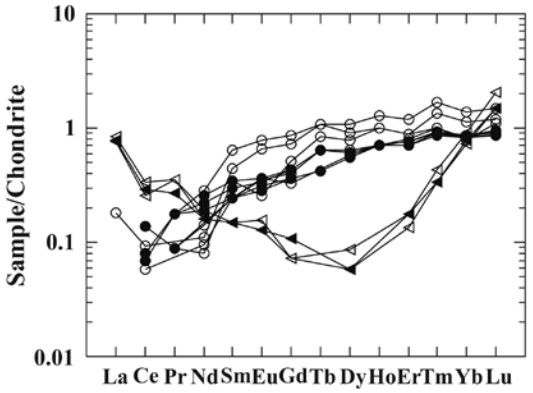

FIG. 6. Chondrite-normalized REE patterns for the peridotites from Iti and Kallidromon. Normalization values after Nakamura (1974). Symbols as in Figure 5.

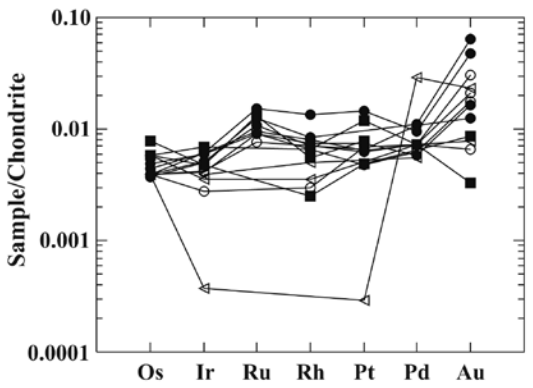

FIG. 7. Chondrite-normalized PGE patterns for ultramafic rocks from Iti and Kallidromon. Normalization values after Naldrett & Duke (1980).

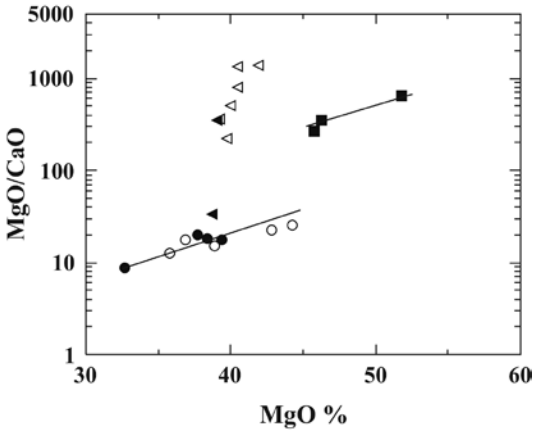

FIG. 8. Variation diagram of MgO *versus* (MgO/CaO), on an anhydrous basis, for ultramafic rocks from Iti and Kallidromon. Symbols as in Figure 5.

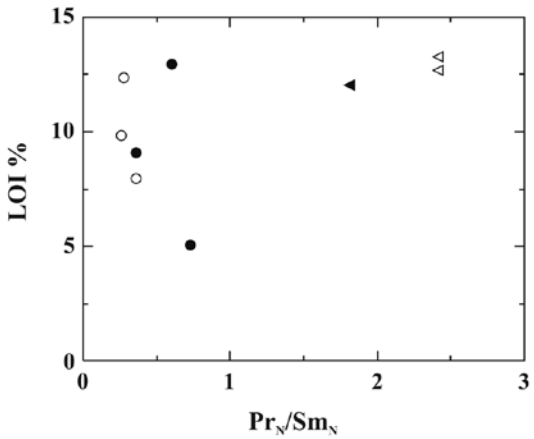

FIG. 9. Variation diagram of Pr_N/Sm_N *versus* Loss On Ignition (LOI), for the Iti and Kallidromon peridotites. Symbols as in Figure 5.

Partial melting processes

The ultramafic rocks from Iti and Kallidromon are highly deformed, and their modal mineralogy is typical of oceanic peridotites and closely resembles that of analogous rocks from the well-known Pindos, Vourinos and Othrys ophiolites. The chemical affinity of the spinels in the lherzolites and the major-element composition of the investigated rocks provide further evidence for their oceanic character. In particular, the low TiO_2/Al_2O_3 values of the ultramafic rocks (up to 0.091, with one exception in sample Kl24, with a value of 1.46) are in the range expected of mid-oceanic peridotites (Menzies 1991). According to experimental data by Mysen & Kushiro (1977), Jaques & Green (1980) and Falloon & Green (1987) this is a consequence of moderate fractionation of Ti relative to Al during the partial melting of peridotites. The TiO_2/Al_2O_3 values in the Iti peridotites also resemble those in the peridotites from Koziakas and Lesvos, whose origins have been assigned to back-arc basins (Migiros *et al*. 2000, Hatzipanagiotou *et al*. 2001).

Strongly refractory peridotites (harzburgites and dunites) found in oceanic or continental lithospheric mantle have usually been interpreted as resulting from high degrees of partial melting of a fertile, homogeneous mantle source (Dick & Bullen 1984, Dick *et al*. 1984, Frey *et al*. 1985, Bodinier 1988, Bodinier *et al*. 1988, Johnson & Dick 1992). The variations shown in Al_2O_3, CaO, V and Ni concentrations (Fig. 5) are similar to what has been reported for several well-known ultramafic rocks in ophiolites world-wide, and demonstrate a partial melting control on the compositions of these rocks and melt extraction from a fertile mantle source. The reasons for the non-existant or weak correlation for many elements may include mobility during

TABLE 5. CHEMICAL COMPOSITION OF ULTRAMAFIC ROCKS FROM ITI (I) AND KALLIDROMON (KL)

	Lherzolites										Harzburgites								Dunites		
	I 126	I 287	I 30	I 617	I 290	Kl 19	Kl 24a	Kl 50	Kl 44	Kl 24	I 189	I 194	I 317	I 389	I 475	I 476	Kl 15	Kl 17	Kl 21	KL 25	Kl 28a
SiO_2 wt%	39.65	39.24	43.08	40.20	46.21	45.58	45.26	41.62	42.09	46.98	41.20	41.03	42.72	41.57	42.05	43.62	43.85	43.09	41.09	41.04	37.33
TiO_2	0.07	0.05	0.05	0.01	0.08	0.34	0.04	0.03	0.04	1.90	0.01	0.01	0.01	0.06	0.01	0.01	0.03	0.09	0.01	0.01	-
Al_2O_3	2.98	2.45	2.41	1.52	1.76	4.71	2.25	1.96	2.10	1.30	0.85	0.77	0.34	0.82	0.86	0.95	1.25	1.07	0.17	0.11	0.05
$Fe_2O_3^t$	8.79	7.59	7.44	7.90	6.96	8.60	8.29	6.89	7.67	6.66	8.93	8.00	8.91	8.18	8.05	8.10	7.70	7.94	8.27	7.87	7.98
MnO	0.11	0.11	0.10	0.11	0.23	0.13	0.12	0.10	0.10	0.14	0.12	0.16	0.10	0.24	0.11	0.10	0.10	0.11	0.11	0.10	0.11
MgO	34.40	38.29	32.54	40.77	32.19	31.14	36.19	34.28	32.60	33.52	34.85	36.22	34.55	34.74	34.35	34.18	34.02	33.73	42.34	42.37	48.90
CaO	2.28	1.67	1.85	1.60	2.57	3.51	2.00	1.91	1.65	0.10	0.03	0.03	0.16	0.04	0.07	0.10	0.10	0.99	0.16	0.12	0.08
Na_2O	0.13	0.11	0.73	0.05	0.04	1.17	0.25	0.18	0.26	-	0.04	0.22	0.07	0.15	0.45	0.04	0.03	0.04	0.33	0.04	0.04
K_2O	0.02	-	0.06	-	0.01	0.10	0.01	0.01	0.01	0.06	0.01	0.02	0.02	0.01	0.02	0.01	0.01	0.01	0.03	0.01	-
P_2O_5	-	-	0.02	-	0.01	0.05	0.01	0.01	0.01	0.14	0.01	0.02	0.09	0.01	0.01	0.01	0.01	0.01	0.01	0.01	-
LOI	12.36	9.84	10.83	7.96	9.90	4.20	5.04	12.44	12.93	9.10	13.27	12.76	12.66	13.84	13.38	12.32	12.10	12.06	6.83	7.75	5.92
Total	100.79	99.35	99.11	100.12	99.96	99.53	99.46	99.43	99.46	99.90	99.32	99.24	99.63	99.66	99.36	99.44	99.20	99.14	99.35	99.43	100.41
Mg#	81.30	84.86	82.93	85.15	83.71	80.09	82.91	84.68	82.53	84.83	81.26	83.42	81.16	82.51	82.58	82.42	83.08	82.52	85.05	85.68	87.19
CaO/Al_2O_3	0.765	0.682	0.768	1.053	1.460	0.745	0.889	0.974	0.786	0.077	0.035	0.039	0.471	0.049	0.081	0.105	0.080	0.925	0.941	1.091	1.60
TiO_2/Al_2O_3	0.023	0.020	0.021	0.007	0.045	0.072	0.018	0.015	0.019	1.462	0.012	0.013	0.029	0.073	0.012	0.011	0.024	0.043	0.059	0.091	-
Ti/V	6.77	7.49	5.26	1.09	7.16	30.88	3.33	2.97	3.87	160.43	1.36	1.42	3.33	7.21	1.34	1.19	3.39	9.30	3.57	4.80	-
Cr ppm	3025	2550	4200	2775	1847	2950	3040	2877	2760	2910	3010	2346	2190	4586	2675	3044	3155	3517	1753	1923	3060
Co	117	102	96	101	*	76	115	92.10	101	113	122	89.40	138	40.30	102.4	114.1	113	*	113.8	105	132
Ni	2204	2185	1750	2080	1476	1280	2045	2025	1880	2030	2220	2225	3200	2108	2388	2617	2550	2267	2540	2634	3061
Cu	34	25	24	23	*	21	29	23.20	16	23	-	17.90	-	12.60	21.10	11	15	41.10	10.60	12.30	12
Zn	67	46	56	85	*	-	77	47.80	46	47	65	53.60	-	53.20	41.50	49.60	50.10	54.40	40.10	40	52
V	62	40	57	55	67	66	72	60.60	62	71	44	42.10	18	49.90	44.60	50.20	53.10	58	16.80	12.50	-
Sr	5	-	3	-	1.80	-	-	2	4	-	-	2	-	2.30	3.70	3.60	3.50	3.30	1.80	3	-
Rb	-	-	-	-	3.30	-	-	1.40	-	-	-	1.50	-	1.30	1.60	1.50	1.40	1.30	1.40	1.50	-
Ba	9	2	-	-	1.60	-	-	1.50	-	-	-	2.10	-	2	7.40	5.80	4.90	3.40	1	2	-
Nb	0.20	-	1.80	0.30	0.10	-	0.80	0.40	-	0.60	1.40	0.20	-	0.20	0.20	0.40	0.40	0.40	0.20	0.20	-
Y	2.50	2	1.80	1.30	1.90	1.40	1.30	2.20	1.40	1.30	-	1.30	-	5.40	1.10	1.20	1.40	2.20	1.20	0.80	-
Sc	14.7	13.3	*	12.4	20.7	*	*	*	*	7.1	*	*	*	*	*	*	*	*	*	*	4
Zr	2	1.50	2	1	2	1	2	1.80	-	2	2	1.50	-	2.50	1.20	7	6	2	2.20	0.30	2.50
Ta	-	-	-	-	0.02	-	-	-	-	0.01	-	0.01	-	-	-	0.01	0.01	-	-	-	-
Hf	-	-	-	-	0.20	-	-	-	-	-	-	-	-	-	-	0.20	0.10	-	-	-	-
Th	-	0.03	-	-	0.10	-	-	-	-	-	-	0.60	-	-	0.08	0.02	0.01	-	-	-	-
U	-	-	0.02	-	*	-	0.01	-	-	0.01	-	-	0.01	0.01	0.02	-	-	-	-	-	-

-: Concentration below detection limit, * not analyzed; Mg# = 100[MgO/(MgO + FeO^t)].

serpentinization or metamorphism, or metasomatism by melt–fluid or melt–rock interaction (*e.g.*, Melcher *et al.* 2002). The Ti/V values in all samples from Iti and Kallidromon range from 1.1 to 9.3, with two exceptions of samples Kl19 (30.9) and Kl24 (160.4), which are rich in TiO_2. The fact that this average value is lower than the chondritic composition, which is at about 10 (Shervais 1982, Briqueu *et al.* 1984), implies the involvement of a partial melting event in the origin of Iti and Kallidromon ultramafic rocks.

The REE contents of the harzburgites, lherzolites, and particularly dunites are low. This is common in ophiolitic mantle rocks that display a depleted character. The lherzolites resemble fertile abyssal peridotites with generally LREE-depleted patterns and almost flat middle and heavy REE profiles. Notably, the Iti lherzolites have relatively high abundances of middle and heavy REE. The observed elemental correlations of most compatible and moderately incompatible elements with MgO abundances (Fig. 5), as well as depletions in the REE and incompatible elements suggest that the lherzolites have undergone a partial melting episode; analogous data have been reported from Frey *et al.* (1985) and Johnson *et al.* (1990). Arai (1987) and Cabanes & Mercier (1988) suggested that primitive mantle peridotites contain olivine with Fo of 87.5–88.0 and spinel with Cr# of 8–10; these values increase with the evolution of partial melting. The higher values of Fo and Cr# in olivine and spinel, respectively, in the studied peridotites (Tables 1, 3), relative to primitive mantle peridotites, are consistent with the imprint of a partial melting episode, even in the most fertile material, the lherzolites. The low Ti contents of clinopyroxenes in the harzburgitic and dunitic rocks (Table 2) are also suggestive of partial melting and depletion, similar to ultramafic rocks from many ophiolites worldwide (*e.g.*, Harris 1995).

TABLE 6. RARE-EARTH-ELEMENT CONCENTRATIONS IN ULTRAMAFIC ROCKS FROM ITI (I) AND KALLIDROMON (KL)

	Lherzolites									Harzburgites		
	I126	I287	I30	I617	I290	Kl19	Kl24a	Kl44	Kl24	I189	I317	Kl17
La	-	-	0.06	-	-	-	-	-	-	0.25	0.28	0.26
Ce	-	-	0.08	-	0.05	-	0.07	0.06	0.12	0.22	0.29	0.25
Pr	0.02	0.01	-	0.01	-	-	0.02	0.02	0.01	0.04	0.04	0.03
Nd	0.18	0.05	0.07	0.09	0.06	0.16	0.12	0.14	-	0.10	0.12	0.10
Sm	0.13	0.07	0.09	0.05	0.05	0.07	0.05	0.06	0.05	0.03	0.03	0.03
Eu	0.06	0.02	0.05	0.03	0.03	0.03	0.02	0.03	0.02	0.01	0.01	0.01
Gd	0.24	0.14	0.20	0.11	0.09	0.12	0.10	0.12	0.10	0.02	0.02	0.03
Tb	0.05	0.04	0.05	0.03	-	0.03	0.02	0.03	0.02	-	-	-
Dy	0.37	0.27	0.31	0.22	0.20	0.21	0.19	0.21	0.19	0.02	0.03	0.02
Ho	0.09	0.07	0.07	0.05	0.05	0.05	0.05	0.05	0.05	-	-	-
Er	0.27	0.20	0.20	0.17	0.18	0.16	0.16	0.17	0.16	0.03	0.04	0.04
Tm	0.05	0.04	0.03	0.03	0.03	0.03	0.03	0.03	0.03	0.01	0.01	0.01
Yb	0.30	0.25	0.18	0.18	0.17	0.18	0.19	0.19	0.19	0.16	0.20	0.17
Lu	0.05	0.04	0.03	0.03	0.04	0.03	0.03	0.03	0.03	0.05	0.07	0.05

-: Concentration (in ppm) below detection limit.

Melt–rock interaction

Harzburgites and dunites have traditionally been viewed as depleted, refractory residues produced by partial melting of more fertile peridotites (Coleman 1977). However, this interpretation does not account for the compositions of our harzburgites, which have well-developed concave-upward REE patterns indicating significant LREE enrichment (Fig. 6), because a simple partial melting process should have produced a LREE-depleted pattern. Such LREE-enriched patterns are now believed to reflect partial melting accompanied by melt–peridotite interaction during melt percolation

TABLE 7. CONCENTRATIONS OF PLATINUM-GROUP ELEMENTS AND Au IN ULTRAMAFIC ROCKS FROM ITI (I) AND KALLIDROMON (KL)

	Lherzolites								Harzburgites			Dunites		
	I126	I30	I617	I290	Kl19	Kl24a	Kl44	Kl24	I189	I317	I475	Kl21	Kl25	Kl28a
Os	2.0	2.0	2.0	2.0	2.3	2.0	1.9	2.5	3.0	2.0	-	3.0	4.0	3.0
Ir	3.3	2.2	2.3	1.5	3.3	2.8	2.7	3.2	1.9	0.2	2.1	3.7	2.6	2.6
Ru	6.5	6.2	5.3	-	10.6	7.5	8.6	6.2	-	-	-	-	9.0	-
Rh	1.6	1.3	1.4	0.6	2.7	1.4	1.7	1.5	0.7	-	1.0	1.3	1.1	0.5
Pt	6.5	4.8	6.3	7.0	14.7	6.7	-	7.6	-	0.3	-	12.0	8.0	5.0
Pd	4.0	3.4	4.0	4.0	5.2	5.9	6.0	3.2	4.0	15.6	3.0	4.0	-	-
Au	3.2	2.7	4.6	1.0	7.3	1.9	9.7	2.5	1.2	3.5	-	0.5	-	1.3
Pd/Ir	1.21	1.55	1.74	2.67	1.58	2.11	2.22	1.00	2.11	78	1.43	1.08	-	-

-: Concentration (in ppb) below detection limit.

processes through the mantle sequence (Edwards 1990, Bodinier *et al*. 1991, Kelemen *et al*. 1992, Suhr *et al*. 1998, Zhou *et al*. 2005). Interaction between ascending magmas and upper-mantle wallrock is enhanced where magma ascends slowly through narrow conduits or by grain-boundary infiltration (Kelemen *et al*. 1990). According to Kelemen *et al*. (1990), and based on different degrees of pyroxene dissolution, three different types of reaction between basaltic magmas and lherzolite can lead to lherzolitic, harzburgitic and dunitic compositions. In more recent studies, Kelemen *et al*. (1995, 1997), and Suhr (1999) have shown that mantle dunites and harzburgites can form from lherzolites during melt percolation processes by clinopyroxene dissolution, incongruent melting of orthopyroxene, and precipitation of olivine from the melt. In such a case, harzburgites can be formed by a melt percolation process with a relatively small melt : rock ratio (Kelemen *et al*. 1992).

The type of melt that reacted with Iti and Kallidromon peridotites (LREE-depleted lherzolites) to form the U-shaped REE patterns of the harzburgites is unlikely to be MORB-type, because such magmas have chondrite-normalized REE patterns depleted in LREE. The most appropriate type of magma, to react with those peridotites would be of boninitic composition because boninites have a U-shaped chondrite-normalized REE pattern (*e.g.,* Crawford *et al*. 1989). The development of subhedral to euhedral grains of Cr-rich spinel, in contrast with the anhedral Al-rich spinel of lherzolitic affinity, and their subsequent evolution toward relatively poorer in Cr compositions, discussed earlier, are also consistent with crystallization induced from a boninitic melt (Leblanc & Ceuleneer 1992). Besides, boninitic melts are known to be S-undersaturated (Keays 1995) and thus were able to remove sulfides from the host rocks to generate the low Cu contents observed in the harzburgites and dunites (Table 5).

Consequently, the formation of the harzburgite can be attributed to the assimilation of pyroxenes by an olivine-saturated melt, intruded from greater depth and injected into the Iti and Kallidromon lherzolite along cracks and fractures (*e.g*., Kelemen 1990a). Melt–rock interaction was driven by the fact that the hydrous boninitic melt, which would have been in equilibrium with the lherzolite at greater depth, was not in equilibrium with the lower-pressure and cooler lherzolite. Upon intrusion, the melt thus reacted with both clinopyroxene and orthopyroxene of the host lherzolite to produce one or all of orthopyroxene, spinel and olivine, hence forming the harzburgite and the dunite (*e.g.,* Kelemen 1990a, b, Kelemen *et al*. 1992). Olivine formation was also enhanced by the presence of H_2O, which expands its stability field at the expense of that of pyroxene (Kushiro 1969, 1972). Chromian spinel may also crystallize during this process, simply because of the enrichment of the residual melt in SiO_2, as olivine crystallizes (Zhou *et al*. 1994, Zhou & Robinson 1997). The component H_2O may also have played an important role to the formation of chromian spinel, as it lowers the liquidus of silicate minerals much more than that of the spinel and thus has the effect of expanding its stability field (Nicholson & Mathez 1991). Consequently, the formation of the harzburgites can be attributed to smaller values of melt : rock ratio and partial assimilation of clinopyroxene or orthopyroxene (or both) from the host lherzolite, relative to the dunites.

On the basis of geochemical data and mainly on trace-element and rare-earth-element contents in clinopyroxene from peridotites, the ophiolite complexes of Vourinos, Pindos and Othrys have been interpreted as being formed (entirely or partially) in an island-arc environment (Pearce *et al*. 1984, Smith & Spray 1984, Bizimis *et al*. 2000). According to Bizimis *et al*. (2000), Dijkstra *et al*. (2001, 2002), Saccani & Photiades (2004), there is abundant evidence that percolating melt played a prominent role in the formation of the Vourinos, Pindos and Othrys peridotites. The percolating melt that refertilized the mantle in a form of a "cryptic metasomatism" probably had a depleted boninitic composition (Bizimis *et al*. 2000, Dijkstra *et al*. 2001), similar to the case at Iti and Kallidromon.

Geotectonic regime

Infiltration of a LREE-enriched boninitic melt is compatible with a supra-subduction-zone melting process, wherein small volumes of slab-derived melts retain their enriched compositions. In fact, a mantle wedge above a subduction zone is considered an ideal site in which boninitic melts are generated (*e.g.,* Plank & Langmuir 1998). The important role of H_2O in the fluid phase inferred for the formation of the harzburgite and dunite provides good evidence for such an environment. Moreover, as emphasized by Kelemen (1990a), subduction environments facilitate melt propagation by porous flow within the mantle wedge, above the Benioff zone, because of volatile release from the subducted slab and inversion of the geothermal gradient. In this situation, volatiles immediately promote first hydrous melting at depths and the hydrous melts, encountering inverted geothermal gradients, can percolate through large volume of mantle rocks.

The high Cr and Ni and the low Al in the ultramafic rocks from Iti and Kallidromon result in high Cr/Al and Ni/Al values. On a Cr/Al *versus* Ni/Al diagram, the Iti and Kallidromon ultramafic rocks follow the same trend and plot at the intermediate part of the trend defined by extremely and less refractory ophiolitic ultramafic rocks (Fig. 10), being similar to samples from Vourinos, which are considered of SSZ origin. The dunites from Kallidromon are plotted at Ni/Al and Cr/Al > 1 (the refractory or arc-type side of the defined trend), the harzburgites are plotted at Ni/Al in the range 0.3–0.6

and Cr/A in the range l 0.4–1. Finally, the lherzolites studied indicate a Ni/Al value from 0.05 to 0.3 and a Cr/Al value from 0.1 to 0.4.

Behavior of the PGE

Previous studies have shown that serpentinization processes do not have any significant effect on PGE ratios, probably because serpentinization occurs in a very reducing environment, and the noble metals are considered to be extremely unreactive under such conditions (Snow & Schmidt 1998, Rehkämper *et al*. 1999a). PGE distribution is predominantly controlled by processes in the mantle, such as partial melting and melt percolation (Büchl *et al*. 2002). In order to resolve the possible effect of melt percolation, the influence of partial melting on the PGE distribution in the source rocks must be evaluated.

During partial melting, Os, Ir and Ru behave compatibly because these elements are included in residual phases, such as sulfides, alloys or oxides (*e.g.,* Mitchell & Keays 1981, Lorand 1989). The concentrations of these metals thus increase in the residue after the extraction of the melt. Furthermore, mantle peridotites and ultramafic melts contain Os and Ir in relatively chondritic abundances, implying that these elements are not significantly fractionated during partial melting (Barnes *et al*. 1985, Brügmann *et al*. 1987, Rehkämper *et al*. 1999b, Lorand *et al*. 2000). However, high-precision data in some peridotites indicate suprachondritic Ru/Ir values (Rehkämper *et al*. 1999a, Lorand *et al*. 2000). If the degree of partial melting does not exceed 20%, the concentrations of Pd, Pt in the residual mantle would increase, because these elements are retained in the residual sulfide phase. At larger degrees of partial melting (>20%), sulfides are consumed by the melt, and Pd, Pt and Re behave incompatibly, whereas Os, Ir and Ru still behave compatibly (*e.g.,* Lorand *et al*. 1999).

Reaction of sulfide phases, which primarily host the PGE, with a percolating silicate melt would mainly control the redistribution of the PGE. The identity of the sulfide phase is important because it has been shown that different sulfide grains have highly variable PGE concentrations and patterns, which could cause severe small-scale heterogeneities with regard to both the absolute and the relative concentrations of PGE (Alard *et al*. 2000, Luguet *et al*. 2001). If PGE variation is controlled by differences in the sulfide phases, then the sulfide distribution reflects the primary fractionation during the percolation event. The amount of mantle sulfides left behind in a mantle channel is controlled by the amount of influxing percolating melt (melt:rock ratio) because the higher the melt flux, the more sulfide can be dissolved and removed. However, as soon as the percolating melt becomes S-saturated, it leaves behind sulfides, which mix with the residual mantle sulfides (Büchl *et al*. 2002).

The fact that the PGE patterns of the residual mantle rocks analyzed (*i.e.,* the harzburgites and the dunites) tend to be slightly enriched in Rh, Pt and Pd relative to Os, Ir and possibly Ru (see Fig. 7, Table 7) rather suggests that melt percolation mobilized and fractionated these elements in contrast to ordinary partial melting. Such an element pattern is typical for rocks affected by mantle-derived melts (*e.g.,* boninite; Brügmann *et al*. 1987). Moreover, the more depleted PGE concentrations in the harzburgite and dunite studied, relative to the lherzolite (Table 7), are compatible with an interaction with boninitic magmas, which are highly S-undersaturated and thus able to remove sulfides from the host rocks (Keays 1995).

The harzburgitic sample I317 shows an anomalous PGE pattern (Fig. 7), displaying extremely low Ir and Pt concentrations and fractionation between Os–Ir and Pt–Pd. The fractionation of PGE even in the same subgroup iridium-group PGE, platinum-subgroup PGE (IPGE, PPGE) is mainly attributed to melt percolation (*e.g.,* Büchl *et al*. 2002). Bezmen *et al*. (1994) also suggested that in H_2O-saturated silicate melts, Ir may become fractionated from Os and Ru because of the large differences of the sulfide–silicate partition coefficients.

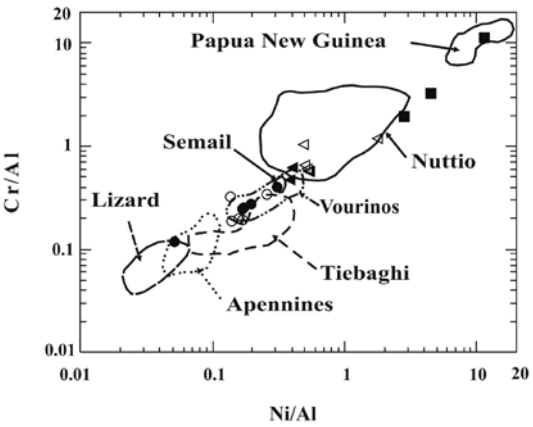

FIG. 10. Cr/Al *versus* Ni/Al plot for ophiolitic mantle rocks from Iti and Kallidromon. Reference data taken from Jaques & Chappell (1980), Roberts & Neary (1993), Rampone *et al*. (1995) and Hanski (1997). Symbols as in Figure 5.

CONCLUSIONS

The ophiolite rocks at Iti and Kallidromon Mountains comprise an incomplete sequence of an ophiolite *mélange* and ultramafic rocks, serpentinized to various degrees. Ultramafic rocks include lherzolite and harzburgite, and dunite lenses that occur within the lherzolite at Kallidromon. These rocks display textures typical of upper mantle tectonites, appropriate for the involve-

ment of partial melting. The geochemical behavior of certain elements further supports the involvement of a partial melting event, at least in the initial stages of the evolution of the peridotites.

The U-shaped REE patterns in the harzburgite, the Cr-rich spinel in both the harzburgite and dunite can be explained by a melt–peridotite interaction episode. The percolating melt is considered to have been of boninitic affinity, generated in a mantle wedge above the subduction zone, and injected into the Iti and Kallidromon lherzolite along cracks and fractures. Melt–rock interaction was driven by the fact that the hydrous boninitic melt, which would have been in equilibrium with the lherzolite at greater depth, was not in equilibrium with the lower-pressure and cooler lherzolite. This melt reacted with both clinopyroxene and orthopyroxene of the host lherzolite to produce one or all of orthopyroxene, Cr-rich spinel and olivine, hence forming the dunite and the harzburgite. Subsequent evolution of spinel compositions relatively poorer in Cr resulted from the normal evolution of the boninitic melt. The formation of the harzburgite can be assigned to smaller melt : rock ratios and partial assimilation of clinopyroxene or orthopyroxene (or both) from the host lherzolite, relative to the dunite. To explain the rather unusual association of dunite pods in the Kallidromon lherzolite, we suggest that the boninitic melts were locally ponded and reacted over a long time with the host lherzolite, increasing their SiO_2 contents by the assimilation of clinopyroxene and orthopyroxene and leading to the precipitation of olivine and Cr-rich spinel. The higher melt-fraction in the dunites was largely modified by melt–rock interaction, thus resulting in spinel compositions richer in Cr, relative to those in the harzburgites. In our opinion, H_2O also played an important role in the formation of the Cr-rich spinel and olivine, in the harzburgite, probably by expanding their fields of stability. The more depleted PGE concentrations in the harzburgite and dunite relative to the lherzolite are consistent with their interaction with highly S-undersaturated boninitic magmas. Therefore, the formation of both the dunite and the harzburgite is interpreted as the result of a multistage history of depletion, deformation and refertilization.

The rocks investigated display considerable similarities with Othrys, Pindos and Vourinos ophiolites, all of SSZ origin. The involvement of a boninitic melt and the significant contribution of H_2O in the formation of the harzburgite and dunite from Iti and Kallidromon, along with geochemical evidence, strongly suggest a subduction-related regime. Therefore, we suggest that these ophiolitic sequences were formed in a marginal basin within the major Pindos oceanic strand.

Acknowledgements

The authors gratefully acknowledge critical reviews of the manuscript by Professor J.-L. Bodinier, as well as by Professor S. Arai and an anonymous referee. Professor J.E. Mungall provided very useful comments, linguistic corrections and editorial handling.

References

Abzalov, M.Z. (1998): Chrome-spinels in gabbro–wehrlite intrusions of the Pechenga area, Kola Peninsula, Russia: emphasis on alteration features. *Lithos* **43**, 109-134.

Alard, O., Griffin, W.L., Lorand, J.P., Jackson, S.E. & O'Reilly, S.Y. (2000): Non-chondritic distribution of the highly siderophile elements in mantle sulfides. *Nature* **407**, 891-894.

Allègre, C.J., Poirier, J.P., Humler, E. & Hofmann, A.W. (1995): The chemical composition of the Earth. *Earth Planet. Sci. Lett.* **134**, 515-526.

Arai, S. (1987): An estimation of the least depleted spinel peridotite on the basis of olivine–spinel mantle array. *Neues Jahrb. Mineral., Monatsh.*, 347-354.

Arai, S. (1994a): Characterisation of spinel peridotites by olivine–spinel compositional relationships: review and interpretation. *Chem. Geol.* **113**, 191-204.

Arai, S. (1994b): Compositional variation of olivine–chromian spinel in Mg-rich magmas as a guide to their residual spinel peridotites. *J. Volcan. Geotherm. Res.* **59**, 279-293.

Barnes, S.J. (2000): Chromite in komatiites. II. Modification during greenschist to mid-amphibolite facies metamorphism. *J. Petrol.* **41**, 387-409.

Barnes, S.J., Naldrett, A.J. & Gorton, M.P. (1985): The origin of the fractionation of platinum-group elements in terrestrial magmas. *Chem. Geol.* **53**, 303-323.

Baumgartner, P.O. (1984): Middle Jurassic – Early Cretaceous low-latitude radiolarian zonation based on Unitary Associations and age of Tethyan radiolarites. *Eclogae Geol. Helv.* **77**, 729-837.

Baumgartner, P.O. & Bernoulli, D. (1976): Stratigraphy and radiolarian fauna in a Late Jurassic – Early Cretaceous section near Achladi (Evvoia, eastern Greece). *Eclogae Geol. Helv.* **69**, 601-626.

Bezmen, N.I., Asif, M., Brügmann, G.E., Romanenko, I.M. & Naldrett, A.J. (1994): Distribution of Pd, Rh, Ru, Ir, Os and Au between sulfide and silicate metals. *Geochim. Cosmochim. Acta* **58**, 1251-1260.

Bizimis, M., Salters, V.J.M. & Bonatti, E. (2000): Trace and REE content of clinopyroxenes from supra-subduction zone peridotites. Implications for melting and enrichment processes in island arcs. *Chem. Geol.* **165**, 67-85.

Bliss, N.W. & MacLean, W.H. (1975): The paragenesis of zoned chromite from central Manitoba. *Geochim. Cosmochim. Acta* **39**, 973-990.

Bodinier, J.L. (1988): Geochemistry and petrogenesis of the Lanzo peridotite body, western Alps. *Tectonophysics* **149**, 67-88.

BODINIER, J.L., DUPUY, C. & DOSTAL, J. (1988): Geochemistry and petrogenesis of eastern Pyrenean peridotites. *Geochim. Cosmochim. Acta* **52**, 2893-2907.

BODINIER, J.L., MENZIES, M.A. & THIRLWALL, M.F. (1991): Continental to oceanic mantle transition: REE and Sr–Nd isotopic geochemistry of the Lanzo lherzolite massif. *J. Petrol.*, Sp. Vol. "Orogenic Lherzolites and Mantle Processes", 191-210.

BONATTI, E. & MICHAEL, P.J. (1989): Mantle peridotites from continental rifts to ocean basins to subduction zones. *Earth Planet. Sci. Lett.* **91**, 297–311.

BRIQUEU, L., BOUGAULT, H. & JORON, J.L. (1984): Quantification of Nb, Ta, Ti and V anomalies in magmas associated with subduction zones: petrogenetic implications. *Earth Planet. Sci. Lett.* **68**, 297-308.

BRÜGMANN, G.E., ARNDT, N.T., HOFMANN, A.W. & TOBSCHALL, H.J. (1987): Noble metal abundances in komatiic suites from Alexo, Canada, and Gorgona Island, Columbia. *Geochim. Cosmochim. Acta* **51**, 2159-2169.

BÜCHL, A., BRÜGMANN, G., BATANOVA, V.G., MÜNKER, C. & HOFMANN, A.W. (2002): Melt percolation monitored by Os isotopes and HSE abundances: a case study from the mantle section of the Troodos Ophiolite. *Earth Planet. Sci. Lett.* **204**, 385-402.

CABANES, N. & MERCIER, J.C.C. (1988): Insight into the upper mantle beneath an active extensional zone: the spinel–peridotite xenoliths from San Quentin (Baja California, Mexico). *Contrib. Mineral. Petrol.* **100**, 374-382.

CAMERON, W.E., NISBET, E.G. & DIETRICH, V.J. (1979): Boninites, komatiites and ophiolitic basalts. *Nature* **280**, 550-553.

CELET, P. (1962): Contribution à l' étude géologique du Parnasse–Kiona et d' une partie des régions méridionales de la Grèce continentale. *Ann. Géol. Pays Hell.* **13**, 446.

CELET, P. (1976): À propos du mélange de type "volcano-sédimentaire" de l'Iti (Grèce méridionale). *Bull. Soc. Géol. Fr.* **18**, 299-307, et Coll. Int. C.N.R.S. Paris, **nº 244**, 103-111.

CELET, P., FERRIÈRE, J. & WIGNIOLLE, E. (1977): Le problème de l' origine des blocs exogènes du mélange à éléments ophiolitiques au Sud du Sperchios et dans le massif de l' Othrys (Grèce). *Bull. Soc. Géol. Fr.* **19**, 935-942.

COLEMAN, R.G. (1977): *Ophiolites: Ancient Oceanic Lithosphere*. Springer, Berlin, Germany.

CRAWFORD, A.J., FALLON, T.J. & GREEN, T.H. (1989): Classification, petrogenesis and tectonic setting of boninites. *In* Boninites and Related Rocks (A.J. Crawford, ed.). Unwin Hyman, London, U.K. (1-49).

DANELIAN, T. & ROBERTSON, A.H.F. (1995): Radiolarian evidence of Middle Jurassic collapse of the Pelagonian carbonate platform (Kallidromon mountains, central Greece). *In* Proc. 15th Congr. Carpatho-Balcan Geol. Assoc. (Athens). *Geol. Soc. Greece, Spec. Publ.* **4**, 175-180.

DEER, W.R., HOWIE, R.A. & ZUSSMAN, J. (1992): *An Introduction to the Rock-Forming Minerals*. Longman, Essex, U.K.

DICK, H.J.B. (1989): Abyssal peridotites, very slow spreading ridges and ocean ridge magmatism. *In* Magmatism in the Ocean Basins (A.D. Saunders & M.J. Norry, eds.). *Geol. Soc., Spec. Publ.* **42**, 71-105.

DICK, H.J.B. & BRYAN, W.B. (1979): Variation of basalt phenocryst mineralogy and rock composition in DSDP hole 396B. *Initial Reports DSDP* **46**, 215-225.

DICK, H.J.B. & BULLEN, T. (1984): Chromian spinel as a petrogenetic indicator in abyssal and Alpine-type peridotites and spatially associated lavas. *Contrib. Mineral. Petrol.* **86**, 54-76.

DICK, H.J.B., FISHER, R.L. & BRYAN, W.B. (1984): Mineralogic variability of the uppermost mantle along mid-ocean ridges. *Earth Planet. Sci. Lett.* **69**, 88-106.

DIETRICH, V.J., OBERHAENSLI, R. & MERCOLLI, I. (1987): A new occurrence of boninite from the ophiolitic mélange in the Pindus – Sub-Pelagonian zone S.L. (Aegina Island, Saronic gulf, Greece). *Ofioliti* **12**, 83-90.

DIJKSTRA, A.H., DRURY, M.R. & VISSERS, R.L.M. (2001): Structural petrology of plagioclase peridotites in the West Othris Mountains (Greece): melt impregnation in mantle lithosphere. *J. Petrol.* **42**, 5-24.

DIJKSTRA, A.H., DRURY, M.R., VISSERS, R.L.M. & NEWMAN, J. (2002): On the role of melt-rock reaction in mantle shear zone formation in the Othris Peridotite Massif (Greece). *J. Struct. Geol.* **24**, 1431-1450.

ECONOMOU-ELIOPOULOS, M., TARKIAN, M. & SAMBANIS, G. (1999): On the geochemistry of chromitites from the Pindos ophiolite complex, Greece. *Chem. Erde* **59**, 19-31.

ECONOMOU-ELIOPOULOS, M. & VACONDIOS, I. (1995): Geochemistry of chromitites and host rocks from the Pindos ophiolite complex, northwestern Greece. *Chem. Geol.* **122**, 99-108.

EDWARDS, S.J (1990): Harzburgites and refractory melts in the Lewis Hills massif, Bay of Island ophiolite complex: the base-metals and precious-metals story. *Can. Mineral.* **28**, 537-552.

EVANS, B.W. & FROST, B.R. (1975): Chrome spinel in progressive metamorphism – a preliminary analysis. *Geochim. Cosmochim. Acta* **39**, 959-972.

FALLOON, T.J. & GREEN, D.H. (1987): Anhydrous partial melting of MORB pyrolite and other peridotite compositions at 10 kbars; implications for the origin of primitive MORB glasses. *Mineral. Petrol.* **37**, 181-219.

FREY, F.A. (1984): Rare earth abundances in upper mantle rocks. *In* Rare Earth Element Geochemistry (P. Henderson, ed.). Elsevier, Amsterdam, The Netherlands (153-203).

FREY, F.A., SUEN, C.J. & STOCKMAN, H.W. (1985): The Ronda high temperature peridotite: geochemistry and petrogenesis. *Geochim. Cosmochim. Acta* **49**, 2469-249. (Pagination?)

GODARD, M., JOUSSELIN, D. & BODINIER, J-L. (2000): Relationships between geochemistry and structure beneath a palaeo-spreading centre: a study of the mantle section in the Oman ophiolite. *Earth Planet. Sci. Lett.* **180**, 133-148.

HANSKI, E.S. (1997): The Nuttio serpentinite belt, central Lapland: An example of Paleoproterozoic ophiolitic mentle rocks in Finland. *Ofioliti* **22**, 35-46.

HARRIS, R.A. (1995): Geochemistry and tectonomagmatic affinity of the Misheguk massif, Brook Range ophiolite, Alaska. *Lithos* **35**, 1-25.

HARTE, B. (1977): Rock nomenclature with particular relation to deformation and crystallization textures in olivine bearing xenoliths. *J. Geol.* **85**, 279-288.

HATZIPANAGIOTOU, K., POMONIS, P. & TSIKOURAS, B. (2001): Origin and evolution of ultramafic rocks from the Koziakas ophiolite, continental Greece. *Braunschweiger geowiss. Arb.* **24**, 235-247.

JAQUES, A.L. & CHAPPELL, B.W. (1980): Petrology and trace element geochemistry of the Papuan ultramafic belt. *Contrib. Mineral. Petrol.* **75**, 55-70.

JAQUES, A.L. & GREEN, D.H. (1980): Anhydrous melting of peridotite at 0–15 kbar pressure and genesis of tholeiitic basalts. *Contrib. Mineral. Petrol.* **73**, 287-310.

JOHNSON, K.T.M. & DICK, H.J.B. (1992): Open system melting and temporal and spatial variation of peridotite and basalt at the Atlantis II fracture zone. *J. Geophys. Res.* **97**, 9219-9241.

JOHNSON, K.T.M., DICK, H.J.B. & SHIMIZU, N. (1990): Melting in the oceanic upper mantle: an ion microprobe study of diopsides in abyssal peridotites. *J. Geophys. Res.* **95**, 2661-2678.

KEAYS, R.R. (1995): The role of komatiitic and picritic magmatism and S-saturation in the formation of the ore deposits. *Lithos* **34**, 1-18.

KELEMEN, P.B. (1990a): Reaction between ultramafic rock and fractionating basaltic magma. I. Phase relations, the origin of calc-alkaline magma series, and the formation of discordant dunite. *J. Petrol.* **31**, 51-98.

KELEMEN, P.B. (1990b): Reaction between ultramafic rock and fractionating basaltic magma. II. Experimental investigation of reaction between olivine tholeiite and harzburgite at 1150–1050°C and 5 kb. *J. Petrol.* **31**, 99-134.

KELEMEN, P.B., DICK, H.J.B. & QUICK, J.E. (1992): Formation of harzburgite by pervasive melt/rock reaction in the upper mantle. *Nature* **358**, 635-641.

KELEMEN, P.B., HIRTH, G., SHIMIZU, N., SPIEGELMAN, M. & DICK, H.J.B. (1997): A review of melt migration processes in the adiabatically upwelling mantle beneath oceanic spreading ridges. *Phil. Trans. R. Soc. Lond.* **A 355**, 283-318.

KELEMEN, P.B., JOHNSON, K.T.M., KINZLER, R.J. & IRVING, A.J. (1990): High-field-strength element depletions in arc basalts due to mantle-magma interaction. *Nature* **345**, 521-524.

KELEMEN, P.B., JOYCE, D.M., WEBSTER, J.D. & HOLLOWAY, J.R. (1990): Calc-alkaline liquids produced by experimental reaction between olivine tholeiite and harzburgite at 1150–1050°C and 5 kb. *J. Petrol.* **31**, 99-134.

KELEMEN, P.B., SHIMIZU, N. & SALTERS, V.J.M. (1995): Extraction of mid-ocean-ridge basalt from the upwelling mantle by focused flow of melt in dunite channels. *Nature* **375**, 747-753.

KUSHIRO, I. (1969): The system forsterite – diopside – silica with and without water at high pressure. *Am. J. Sci.* **267A**, 269-294.

KUSHIRO, I. (1972): Effect of water on the composition of magmas formed at high pressures. *J. Petrol.* **13**, 311-334.

LEAKE, B.E., WOOLLEY, A.R., ARPS, C.E.S., BIRCH, W.D., GILBERT, M.C., GRICE, J.D., HAWTHORNE, F.C., KATO, A., KISCH, H.J., KRÌVOVICHEV, V.G., LINTHOUT, K., LAIRD, J., MANDARINO, J., MARESCH, W.V., NICKEL, E.H., ROCK, N.M.S., SCHUMACHER, J.C., SMITH, D.C., STEPHENSON, N.C.N., UNGARETTI, L., WHITTAKER, E.J.W. & YOUZHI, G. (1997): Nomenclature of amphiboles: report of the subcommittee on amphiboles of the International Mineralogical Association Commission on new minerals and mineral names. *Mineral. Mag.* **61**, 295-321.

LEBLANC, M. & CEULENEER, G. (1992): Chromite crystallisation in multicellular magma flow: evidence from a chromitite dike in the Oman ophiolite. *Lithos* **27**, 231-257.

LELUC, H. (1978): Contribution à l'étude géologique du Massif du Kallidromon (Grèce continentale). D.E.A., Univ. Lille, Lille, France.

LENSCH, G. (1968): Der normative Mineralbestand von Mafiten. *Neues Jahrb. Mineral., Monatsh.*, 306-320.

LORAND, J.P. (1989): Abundance and distribution of Cu–Fe–Ni sulfides, sulfur, copper and platinum-group elements in orogenic-type spinel lherzolite massifs of Ariege (northeastern Pyrenees, France). *Earth Planet. Sci. Lett.* **93**, 50-64.

LORAND, J.P., GROS, M. & PATTOU, L. (1999): Fractionation of platinum-group element in the upper mantle: a detailed study in Pyrenean orogenic peridotites. *J. Petrol.* **40**, 951-987.

LORAND, J.P., SCHMIDT, G., PALME, H. & KRATZ, K.L. (2000): Highly siderophile element geochemistry of the Earth's mantle: new data for the Lanzo (Italy) and Ronda (Spain) orogenic peridotite bodies. *Lithos* **53**, 149-164.

LUGUET, A., ALARD, O., LORAND, J.P., PEARSON, N.J., RYAN, C. & O'REILLY, S.Y. (2001): Laser-ablation microprobe (LAM–ICPMS) unravels the HSE geochemistry of the oceanic mantle. *Earth Planet. Sci. Lett.* **189**, 285-294.

MCDONOUGH, W.F. & SUN, S.S. (1995): The composition of the Earth. *Chem. Geol.* **120**, 223-253.

MCINNES, B.I.A., GREGOIRE, M., BINNS, R.A., HERZIG, P.M. & HANNINGTON, M.D. (2001): Hydrous metasomatism of oceanic sub-arc mantle, Lihir, Papua New Guinea: petrology and geochemistry of fluid-metasomatised mantle wedge xenoliths. *Earth Planet. Sci. Lett.* **188**, 169-183.

MELCHER, F., MEISEL, T., PUHL, J. & KOLLER, F. (2002): Petrogenesis and geotectonic setting of ultramafic rocks in the Eastern Alps: constraints from geochemistry. *Lithos* **65**, 69-112.

MENZIES, M. (1991): Oceanic peridotites. *In* Oceanic basalts (P.A. Floyd, ed.). Blackie, Glasgow, U.K. (363-385).

MERCIER, J.C.C. & NICOLAS, A. (1975): Textures and fabrics of the upper mantle peridotites as illustrated by basalt xenoliths. *J. Petrol.* **16**. 454-487.

MIGIROS, G., HATZIPANAGIOTOU, K., GARTZOS, E., SERELIS, K. & TSIKOURAS, V. (2000): Petrogenetic evolution of ultramafic rocks from Lesvos Island (NE Aegean, Greece). *Chem. Erde* **60**, 27-46.

MITCHELL, R.H. & KEAYS, R.R. (1981): Abundance and distribution of gold, palladium and iridium in some spinel and garnet lherzolites: implications for the nature and origin of precious metal-rich intergranular components in the upper mantle. *Geochim. Cosmochim. Acta* **45**, 2425–2442.

MORIMOTO, N., FABRIES, J., FERGUSON, A.K., GINZBURG, I.V., ROSS, M., SEIFERT, F.A., ZUSSMAN, J., AOKI, K. & GOTTARDI, G. (1988): Nomenclature of pyroxenes. *Am. Mineral.* **73**, 1123-1133.

MYSEN, B.O. & KUSHIRO, I. (1977): Compositional variations of coexisting phases with degree of partial melting of peridotite in the upper mantle. *Am. Mineral.* **62**, 843-865.

NAKAMURA, N. (1974): Determination of *REE*, Ba, Fe, Mg, Na and K in carbonaceous and ordinary chondrites. *Geochim. Cosmochim. Acta* **38**, 757-773.

NALDRETT, A.J. & DUKE, J.M. (1980): Platinum metals in magmatic sulfide ores. *Science* **208**, 1417-1424.

NICHOLSON, D.M. & MATHEZ, E.A. (1991): Petrogenesis of the Merensky Reef in the Rustenburg section of the Bushveld Complex. *Contrib. Mineral. Petrol.* **107**, 293-309.

O'HANLEY, D.S. (1996): *Serpentinites* (*Records of Tectonic and Petrological History*). Oxford University Press, New York, N.Y.

PAPANIKOLAOU, D. (1989): Are the medial crystalline massifs of the Eastern Mediterranean drifted Godwanian fragments? *Geol. Soc. Greece*, *Spec. Publ.* **1**, 63-90.

PAPASTAMATIOU, J., VETOULIS, D. & TATARIS, A. (1962): Kallidromon. Géologie et corrélation avec le Parnasse. *Ann. Géol. Pays. Hell.* **5**, 43-51.

PAPIKE, J.I., CAMERON, K.L. & BALDWIN, K. (1974): Amphiboles and pyroxenes: characterization of other than quadrilateral components and estimates of ferric iron from microprobe data (abstract). *Geol. Soc. Am., Abstr. Programs* **6**, 1053-1054.

PEARCE, J.A., BARKER, P.F., EDWARDS, S.J., PARKINSON, I.J. & LEAT, P.T. (2000): Geochemistry and tectonic significance of peridotites from the South Sandwich arc-basin system, South Atlantic. *Contrib. Mineral. Petrol.* **139**, 36-53.

PEARCE, J.A., LIPPARD, S.J. & ROBERTS, S. (1984): Characteristics and tectonic significance of supra-subduction zone ophiolites. *In* Marginal Basin Geology (B.P. Kokelaar & M.F. Howells, eds.). *Geol. Soc. Lon.*, Spec. Publ. **14**, 77-93.

PLANK, T. & LANGMUIR, C.H. (1998): The chemical compositions of subducting sediments and its consequences for the crust and mantle. *Chem. Geol.* **145**, 325-394.

RAMPONE, E., HOFMANN, A.W., PICCARDO, G.B. & VANNUCCI, R. (1995): Petrology, mineral and isotope geochemistry of the external Liguride peridotites (northern Apennines, Italy). *J. Petrol.* **36**, 81-105.

REHKÄMPER, M., HALLIDAY, A.N., ALT, J., FITTON, J.G., ZIPFEL, J. & TAKAZAWA, E. (1999a): Non-chondritic platinum-group element ratios in oceanic mantle lithosphere: petrogenetic signature of melt percolation? *Earth Planet. Sci. Lett.* **172**, 65-81.

REHKÄMPER, M., HALLIDAY, A.N., FITTON, J.G., LEE, D.C., WIENEKE M. & ARNDT, N.T. (1999b): Ir, Ru, Pt, and Pd in basalts and komatiites: new constraints for the geochemical behavior of the platinum-group elements in the mantle. *Geochim. Cosmochim. Acta* **63**, 3915-3934.

RICHTER, D., MIHM, A. & MÜLLER, C. (1997): Die pelagonischen Deckenreste auf dem Flysch des Ostpindos-Synklinoriums (Pindos-Zone) westlich des Iti-Gebirges (Mittelgriechenland). *Z. dt. Geol. Ges.* **148**, 237-246.

ROBERTS, S. & NEARY, C. (1993): Petrogenesis of ophiolitic chromitite. *In* Magmatic Processes and Plate Tectonics (H.M. Prichard, T. Alabaster, N.B. Harris & C.R. Neary, eds.). *Geol. Soc. London*, *Spec. Publ.* **76**, 257-272.

ROEDER, P.L. (1994): Chromite: from the fiery rain of chondrules to the Kilauea Iki lava lake. *Can. Mineral.* **32**, 729-746.

SACCANI, E. & PHOTIADES, A. (2004): Mid-ocean ridge and supra-subduction affinities in the Pindos ophiolites (Greece): implications for magma genesis in a forearc setting. *Lithos* **73**, 229-253.

SHERVAIS, J.W. (1982): Ti–V plots and petrogenesis of modern and ophiolitic lavas. *Earth Planet. Sci. Lett.* **59**, 101-118.

SHIGA, Y. (1987): Behavior of iron, nickel, cobalt and sulfur during serpentinisation, with reference to Hayachine ultramafic rocks of the Kamaishi mining district, Northeastern Japan. *Can. Mineral.* **25**, 611-624.

SMITH, A.G. & SPRAY, J.G. (1984): A half-ridge transform model for the Hellenic–Dinaric ophiolites. *In* The Geological Evolution of the Eastern Mediterranean (J.E. Dixon & A.H.F. Robertson, eds). *Geol. Soc. London, Spec. Publ.* **17**, 629-644.

SNOW, J.E. & SCHMIDT, G. (1998): Constraints on Earth accretion deduced from noble metals in the oceanic mantle. *Nature* **391**, 166-169.

STAMPFLI, G.M. (1996): The Intra-Alpine terrain: a Paleotethyan remnant in the Alpine Variscides. *Eclogae geol. Helv.* **89**, 13-42.

STAMPFLI, G.M., MOSAR, J., DE BONO, A. & VAVASSIS, I. (1998): Late Paleozoic, Early Mesozoic plate tectonics of the western Tethys. Eighth Int. Congress, Geol. Soc. of Greece **32**, 113-120.

SUHR, G. (1999): Melt migration under oceanic ridges: inferences from reactive transport modelling of upper mantle hosted dunites. *J. Petrol.* **40**, 575-599.

SUHR, G., SECK, H.A., SHIMIZU, N. & GUNTHER, D. (1998): Infiltration of refractory melts into the lowermost oceanic crust: evidence from dunite- and gabbro-hosted clinopyroxenes in the Bay of Islands ophiolite. *Contrib. Mineral. Petrol.* **131**, 136-154.

WIGNIOLLE, E. (1977): Données nouvelles sur la géologie du massif de l'Iti (Grèce continentale). *Ann. Soc. Géol. Nord.* **47**, 239-251.

ZHOU, M.-F. & ROBINSON, P.T. (1997): Origin and tectonic environment of podiform chromite deposits. *Econ. Geol.* **92**, 259-262.

ZHOU, M.-F., ROBINSON, P.T. & BAI, W.J. (1994): Formation of podiform chromitites by melt/rock interaction in the upper mantle. *Mineral. Deposita* **29**, 98-101.

ZHOU, M.-F., ROBINSON, P.T., MALPAS, J., EDWARDS, S.J. & QI, L. (2005): REE and PGE geochemical constraints on the formation of dunites in the Luobusa Ophiolite, southern Tibet. *J. Petrol.* **46**, 615-639.

ZHOU, M.-F., ROBINSON, P.T., MALPAS, J. & LI, Z. (1996): Podiform chromitites in the Luobusa ophiolite (southern Tibet): implications for melt–rock interaction and chromite segregation in the upper mantle. *J. Petrol.* **37**, 3-21.

ZHOU, M.-F., SUN, M., KEAYS, R.R. & KERRICH, R. (1998): Controls on platinum-group elemental distributions of podiform chromitites: a case study of high-Cr and high-Al chromitites from Chinese orogenic belts. *Geochim. Cosmochim. Acta* **62**, 677-688.

Received